UiT
THE ARCTIC
UNIVERSITY
OF NORWAY

Faculty of Science and Technology

Department of Engineering and Safety IVT

Prediction of ship icing in Arctic waters

Observations and modelling for application in operational weather forecasting

—

Eirik Mikal Samuelsen

A dissertation for the degree of Philosophiae Doctor – June 2017

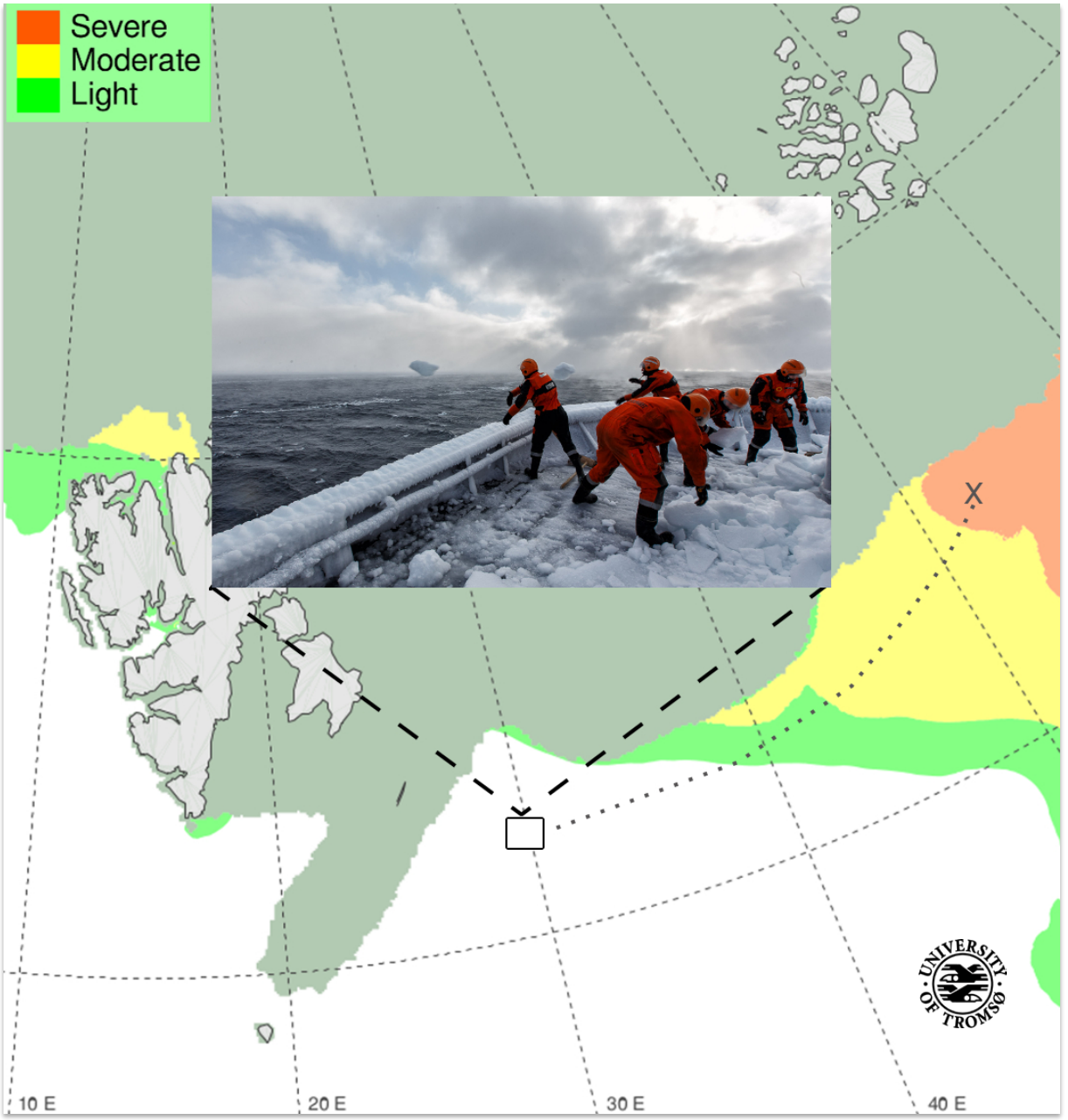

Prediction of ship icing in Arctic waters

Observations and modelling for application in operational weather forecasting

By
Eirik Mikal Samuelsen

Thesis submitted in fulfilment of the requirements for the degree of Doctor of Philosophy (PhD)

Faculty of Science and Technology
Department of Engineering and Safety - IVT
June 2017

Front-page illustration:

Icing forecast based on the Marine Icing model for the Norwegian COast Guard (MINCOG) with input variables from numerical prediction models of the atmosphere (Arome Arctic 2.5 km), the ocean waves (My Wave 4 km), and the ocean (Nordic 4 km). The illustration demonstrates a short-term forecast of icing severity in the Barents Sea for a day in March 2017. The photo is provided by The Norwegian Army/Håkon Kjølmoen, and is an illustration of soldiers on KV Svalbard removing ice after an icing episode in the Barents Sea in the same month. Ice was building up in the front part of the ship despite the fact that the ship is equipped with heating cables. The x, dotted line, and square are illustrating a presumable position of the ship during the icing event, the possible route, and the position afterwards. Since the actual position and timing of the event are unknown, these graphical elements are fictitious and only generated for illustration purposes. The dark-grey filled colour describes the areas with sea ice or the areas in which the input parameters of the icing model are not defined.

...dedicated to my wife Charlotte, and my children Isak, Emil, and Thea, in addition to my beloved parents Ragnar and Walborg.

Then the Lord answered Job from the storm.
He said:
Who is the mother of the ice?
Who gives birth to the frost from the sky,
when the water becomes hard as stone,
and even the surface of the ocean is frozen?"
(Job. 38.1, 29-30)

Abstract

A ship travelling in sub-freezing conditions may encounter sea spray, rain, fog or snow freezing onto various parts of it. Such ship icing is a well-known threat for those individuals who have served on ships operating in a cold marine climate. As de-icing techniques may be energy consuming, accurate prediction of icing is also desirable from a financial point of view. Throughout the last 60 years there have been several efforts trying to model this elusive phenomenon. However, the lack of accurate field observations poses questions to the accuracy of the state-of-the-art modelling approaches including the parameterization of the physical processes of the models. As a consequence, the current study presents and utilises icing data obtained from ship observations in Arctic-Norwegian waters supplemented with high-resolution reanalysis data. On the basis of a unique data set derived from observations recorded on a particular ship type of the Norwegian Coast Guard, a completely new icing model has been developed. Verification of this Marine Icing model for the Norwegian COast Guard (MINCOG) and comparison to currently-applied methods in operational weather forecasting, reveals higher accuracy of MINCOG compared to the other methods. Furthermore, the study stresses the importance of including wave information separately into marine-icing models rather than incorporating it in the wind-speed parameter. A major finding of the study is that nature dictates an upper limit to the degree of icing that may arise from wave-ship interactions, since high waves and very low air temperatures rarely coexist. It is also highlighted that the inclusion of snow may be important for ship icing to transpire, and that icing ensues most frequently during cold-air outbreaks from the ice. In addition, when a more general approach is applied to the icing problem, a prediction method utilising the temperature at 850 hPa provides a potential for forecasting icing several days or weeks ahead in time. The prediction models presented in this study may be incorporated in an ensemble prediction system (EPS) providing the officer of a ship an early warning about the risk of icing and the probability of an expected growth rate of icing.

Sammendrag

Et skip som beveger seg i omgivelser med temperaturer under 0 grader, kan oppleve at sjøsprøyt, regn, tåke eller snø fryser på ulike deler av skipet. Slik skipsising er en velkjent trussel for de som har jobbet på skip som opererer i et kaldt maritimt klima. Siden avising kan være energikrevende, er nøyaktig isingsvarsling ønskelig også fra et økonomisk ståsted. I løpet av de siste 60 årene har det vært mange forsøk på å modellere dette kompliserte fenomenet, men mangelen på gode feltobservasjoner gjør at man må stille spørsmål ved nøyaktigheten til dagens modelleringsmetoder inkludert parameteriseringen av modellenes fysiske prosesser. Som en følge av dette presenterer og anvender dette studiet isingsdata fremkommet av skipsobservasjoner fra Arktisk-Norske farvann. Med utgangspunkt i et unikt datasett utledet av observasjoner utført på en bestemt skipstype fra Den norske Kystvakt, har en helt ny isingsmodell blitt utviklet. Verifikasjon av denne maritime isingsmodellen for Den norske Kystvakt (MINCOG), og sammenligning med andre metoder brukt i operasjonell værvarsling, avslører at MINCOG verifiserer bedre enn de andre metodene. Videre understreker studien viktigheten av å inkludere bølgeinformasjon separat i isingsmodeller brukt over sjø, og ikke inkludert som en del av vindstyrken. Et hovedfunn i studien er at naturen setter en øvre begrensning for mengden ising som kan oppstå på grunn av bølge-skip interaksjoner fordi høye bølger og veldig lave lufttemperaturer sjeldent opptrer samtidig eller i de samme områdene. Det er også fremhevet at snø kan være en viktig faktor for at ising skal kunne forekomme, og at ising oppstår hyppigst i forbindelse med kaldluftsutbrudd fra isen. Hvis man bruker en overordnet tilnærming til isingsproblematikken, vil en prediksjonsmetode som utnytter temperaturen i 850 hPa, gi et potensiale for å varsle ising dager eller uker framover i tid. Prediksjonsmodellene som presenteres i studien kan bli inkludert i et ensemblevarslingssystem (EPS) som kan gi en skipsoffiser et tidlig forvarsel om risikoen for ising og en sannsynlighet for forventet isingshastighet.

Acknowledgements

First and foremost I want to thank my beloved wife Charlotte and our three children Isak, Emil, and Thea for your patience with me during this PhD-period. A lot of things have been put on hold due to the work load and effort demanded for this study to be accomplished. Without your contribution and willingness to cooperate in daily life, this study would never have been fulfilled.

Secondly I have to thank my supervisors Associate Professor Kåre Edvardsen and Professor Rune Grand Graversen for all your help and effort during this period. In particular for providing me with backup and support, fruitful discussions, guidelines, and not least, Kåre, for giving me the opportunity to follow my meteorological ideas. In addition Rune, without your diligent reading and crucial language correction the result would have been considerably degraded. Helpful language correction that should be praised has also been given to me by my sister Reidun Samuelsen Roberts and her husband Andrew Roberts.

I would also like to give a special gratitude to the fellow PhD Candidates, researchers, and friends across several institutes at the Technology Building at UiT - The Arctic University of Norway: Masoud Naseri, Yonas Ayele, Jaap van Rijckevorsel, Bjarte Røed, Taimur Rashid, Alena Dekhtyareva, Rezgar Zaki, Bengt Magne Svendsen, Oddmar Eiksund, Associate Professor Eivind Brodal, Associate Professor Hassan Abbas Khawaja, Brian Murray, Per Roald Leikanger, Sindre Markus Fritzner, and Patrick Stoll. Oddmar Eiksund in particular for several interesting and sometimes challenging discussions and ideas, and for helping me out with several mathematical problems for instance the trajectory model implemented in MINCOG, Alena Dekhtyareva for translating the Russian typewritten article of Kachurin *et al.* (1974) to Norwegian, and Masoud Naseri for letting me share office with him during the last year. It has also been a pleasure to get to know the rest of the colleagues at IIS and IIS-IVT, specifically during our trip to Vilnius and London. The staff at the library of UiT must also be acknowledged since you always throughout this period has been kind and willing to help me out in finding papers not electronically available.

Moreover, I would like to acknowledge my co-supervisor Assoicate Professor Etsuro Shimizu for the kindness shown to us during our visit to Tokyo University of Marine Science And Technology (TUMSAT), and the TUMSAT students Shinya Sasaki and Kyohei Takahata for helping me out with translating the articles Sawada (1962) and Sawada (1967) written in Japanese.

A final gratitude is also provided to all colleagues at the Norwegian Meteorological Institute that have helped me out with challenges of various kinds during the study, in particular Hilde Haakenstad, Ole Johan Aarnes, Dag Kvamme, Heiko Klein, Lisbeth Bergholt, and Signe Aaboe. Other colleagues, family, friends, and fellow researchers that have helped me out, but are not mentioned in this paragraph, are also provided with the highest acknowledgements and you are not forgotten.

Eirik Mikal Samuelsen

Tromsø, Norway

June, 2017

Abbreviations

CFD	-	Computational Fluid Dynamics
ECMWF	-	European Centre for Medium-ranged Weather Forecasts
EPS	-	Ensemble Prediction System
ERA-Interim	-	Global atmospheric reanalysis from ECMWF (Dee *et al.*, 2011)
HIRLAM	-	HIghResolution Limited Area Model
GFS	-	Global Forecast System (NCEP, 2017)
GMSS	-	Gandin-Murphy Skill Score (categorical verification score)
HSS	-	Heidke Skill Score (categorical verification score)
KVN	-	KV Nordkapp ship class data set (Paper II)
M1, M2, M3	-	Modified Stallabrass models applied in Paper I
MFV	-	Medium-sized Fishing Vessel
MINCOG	-	Marine Icing model for the Norwegian COast Guard
MINCOG adj	-	Adjustment of the MINCOG model with a different spray-flux formulation than the original model.
MINCOG adj ro	-	The MINCOG adj model considering spray-water run off in the thermodynamics.
MINCOG adj sn	-	The MINCOG adj model including the effect of snow.
NOAA	-	National Oceanic and Atmospheric Administration
NORA10	-	NOrwegian ReAnalysis 10 km data (Reistad *et al.*, 2011)
O1, O2, O3	-	Overland models applied in Paper I
PC	-	Percent Correct (categorical verification score)
P&C	-	Data set from Pease and Comiskey (1985)
PDF	-	Probability Density Function
PSS	-	Peirce Skill Score (categorical verification score)
R&M	-	Data set from Roebber and Mitten (1987)
ROMS	-	Regional Oceanic Modeling System (Shchepetkin and McWilliams, 2005)
SVIM	-	Nordic Seas 4 km hindcast (Lien *et al.*, 2013)
T1, T2, T3	-	Test models applied in Paper I
WAM	-	WAve Model (Günther *et al.*, 1992)
ZLH	-	Data set from the work of Zakrzewski, Lozowski, and Horjen in Zakrzewski *et al.* (1989)

Nomenclature

A	Albedo of freezing surface (0.56)
a_{ro}	Run-off parameter which may be added to the thermodynamics (0.25)
BIAS	Mean error: $\frac{1}{n'}\sum_{i=1}^{n'}(P_i - O_i)$, n' number of events, P_i predictions, O_i observations
C_I	Sea-ice concentration (area fraction)
c_p	Specific heat capacity of air (1004 J kg^{-1} °C^{-1})
c_s	Specific heat capacity of snow (2×10^3 J kg^{-1} °C^{-1}, Curry and Webster (1999))
c_w	Specific heat capacity of sea water (4×10^3 J kg^{-1} °C^{-1}, Curry and Webster (1999))
D	Width of plate in which icing is observed (4 m)
e_s	Saturation vapour pressure (hPa)
E_S	Total ice accumulation (cm)
f	Function applied to incorporate the effect of run-off water in the thermodynamics (Section 2.3.7)
h	Ice thickness (cm or m)
dh/dt	Icing rate (cm h^{-1})
h_a	Heat-transfer coefficient (W m^{-2} °C^{-1})
h_e	Evaporative heat-transfer coefficient (W m^{-2} hPa^{-1})
H_s	Significant wave height (m)
I_S	Icing cause (code)
k_i	Conductivity of saline-water ice (W m^{-1} °C^{-1})
k^*	Interfacial distribution coefficient (0.3)
L_{fs}	Latent heat of freezing of saline water (J kg^{-1})
L_v	Latent heat of vaporisation (2.5×10^6 J kg^{-1})
$\downarrow\uparrow$ LW	Incoming and outgoing longwave radiation (W m^{-2})
l_{wc}	Liquid water content in spray (kg m^{-3})
l_{wcsnow}	Water equivalent content in snow (kg m^{-3})
MAE	Mean-absolute error: $\frac{1}{n'}\sum_{i=1}^{n'}\lvert P_i - O_i\rvert$
MASE	Mean-absolute-scaled error: $\mathrm{MAE}\times\left(\frac{1}{n'-1}\sum_{i=2}^{n'}\lvert O_i - O_{i-1}\rvert\right)^{-1}$
MSLP	Air pressure at mean sea level (hPa)
N	Spray frequency (s^{-1})
n	Freezing fraction (R_i/R_w or $R_i/(R_w + R_{\mathrm{snow}})$)
N_N	Total cloud cover (oktas)
$\mathbf{n_1}$	Normal vector towards freezing plate
P_P	Water equivalent precipitation intensity (mm s^{-1} or kg m^{-2} s^{-1})
P_s	Significant wave period (s)

Q	Heat flux (W m^{-2}) (Section 2.3.2 for detailed explanation of the various heat fluxes)
r	Correlation coefficient
r_a	Recovery factor for a vertical plate (0.95)
Re	Reynolds number
Ri	Richardson number
R_i	Ice accretion flux (kg m^{-2} s^{-1})
R_H	Relative humidity of air (fraction)
RMSE	Root-mean-squared error: $\sqrt{\frac{1}{n'}\sum_{i=1}^{n'}(P_i - O_i)^2}$
RMSSE	Root-mean-squared-scaled error: $\text{RMSE} \times \left(\frac{1}{n'-1}\sum_{i=2}^{n'}(O_i - O_{i-1})^2\right)^{-1/2}$
R_R	Accumulated precipitation (mm or kg m^{-2})
R_S	Visually-estimated icing rate (code)
R_{snow}	Water equivalent flux from snow (kg m^{-2} s^{-1})
R_w	Spray flux (kg m^{-2} s^{-1})
s	Distance from freezing plate to the gunwale or the perimeter of the ship viewed from above (m)
S_b	Salinity of brine (ppt)
S_i	Salinity of ice (ppt)
S_w	Salinity of incoming sea water (ppt)
$\downarrow\uparrow$ SW	Incoming and reflected shortwave radiation (W m^{-2})
SST	Sea-surface temperature (°C)
$T_a{}^{\dagger}$	Air temperature (°C)
T_{ro}	Temperature of the run-off water when leaving the accretion (°C)
T_s	Surface temperature of the freezing brine (°C)
T_{struct}	Temperature of structure where ice adhere (°C)
Δt	Time difference between two junctures of observations (s or h)
t_{dur}	Duration time of spray clouds (s)
$V^{\dagger}$	Wind speed (m s^{-1})
$\mathbf{V_d}$	Droplet velocity in coordinate system following the ship (m s^{-1} and direction)
V_f	View factor of the incoming shortwave radiation according to the surface in consideration
V_{gr}	Relative speed between the ship and wave groups (m s^{-1})
V_r	Relative speed between the ship and wave phases (m s^{-1})
V_s	Ship speed (m s^{-1})
$\mathbf{V_{snow}}$	Snow velocity in coordinate system following the ship (m s^{-1} and direction)
V_t	Terminal speed of snow flakes (1.7 m s^{-1})
w_0	Constant in l_{wc}-formulation

$w_{1,2}$	Weighting of the along-flow and cross-flow components of the heat-transfer coefficient (h_a)
W_r	Relative speed between the ship and wind or wind speed in coordinate system following the ship (m s^{-1})
W_W	Present weather (code)
z	Height above sea level (6.5-8.5 m)
z_0	Surface roughness
α	Angle between the ship course and the wave direction (°)
β	Angle between the ship course and the wind direction (°)
Δ	Anomaly value of a certain parameter applying monthly mean values of the same parameter
γ	Tilt angle between the freezing plate and the horizontal (85 °)
λ	Wave length (m)
ρ_i	Density of the ice accretion (890 kg m^{-3})
σ	Stefan-Boltzmann constant (5.67×10^{-8} W m^{-2} K^{-4})

Subscripts for variables at different elevations or in different coordinate systems

†	At ship level if no other subscripts are applied.
2m	At 2 m height
10m	At 10 m height
850	At 850 hPa level
x	Along the bow direction in a coordinate system following the ship (Fig.3 in Paper II)
y	Normal to the bow direction in a coordinate system following the ship (Fig.3 in Paper II)

List of appended papers

Paper I **Samuelsen, E. M.**, Løset, S., Edvardsen, K. 2015. "Marine icing observed on KV Nordkapp during a cold air outbreak with a developing polar low in the Barents Sea." In *Proceedings of the 23rd International Conference on Port and Ocean Engineering under Arctic Conditions*, Norwegian University of Science and Technology, Trondheim, 1-14.
URL `http://www.poac.com/Papers/2015/pdf/poac15Final00087.pdf`

Paper II **Samuelsen, E. M.**, Edvardsen, K., Graversen, R. G. 2017. "Modelled and observed sea-spray icing in Arctic-Norwegian waters." *Cold Regions Science and Technology*; **134:** 54-81. doi:`https://doi.org/10.1016/j.coldregions.2016.11.002`

Paper III **Samuelsen, E. M.**. 2017. "Ship-icing prediction methods applied in operational weather forecasting." *Quarterly Journal of the Royal Meteorological Society*; (under second review by May 2017)

Paper IV **Samuelsen, E. M.**, Graversen, R. G. 2017. "Weather situation during observed ship-icing events off the coast of Northern Norway and the Svalbard archipelago." *Tellus A: Dynamic Meteorology and Oceanography*; (submitted May 2017)

Contents

Part I
Summary of thesis

1 Introduction

1.1 Background

Shipping in the Arctic region has for centuries been considered as precarious (Panov, 1978). Although stormy weather conditions and high waves may be encountered in sea areas all over the world, there is an additional potential of ship-borne sea water, in conjunction with or without atmospheric water sources, freezing on a ship in a cold marine climate. Ice build-up above deck level will raise the centre of gravity of the vessel, which may lead to destabilization, and in a worst considerable scenario, capsizing, submerging, and the loss of lives (Shellard, 1974). Most likely icing is the cause of many of the fishing-related calamities experienced at sea off the coast of Northern Norway in the past centuries. One such tragedy is described in detail by Petter Dass in his famous poem "Nordlands Trompet" (The trumpet of Nordland). Dass operated as priest in the southern part of Northern Norway in the end of the 17th and the beginning of the 18th century. He estimates that more than 500 men perished in this disastrous event, and he has the following statement about the reason for the disaster (Erichsen, 1892):

"Men Sagen, at Veiret langt haardere her
End andensteds falder, det voldendes er
Den poliske Circul hin kolde;
Thi dersom ei Landet laa Polen saa nær,
fornam man i Sandhed et mildere Veir."
Petter Dass (1647-1707)

In English translation it would be something like this (without the rhyme):

"But the Issue, that the Weather is much tougher here
Than elsewhere, is the cause of
The cold Polar Circle (or Circulation);
However, if the Region was not situated as close to the Pole,
truly one would experience milder Weather."

Although this particular calamity may not have been directly related to icing, it is interesting to notice that Dass links the challenging weather conditions with his location in the Arctic region.

Yet the ships of today are more seaworthy than those in the 17th century, the perils related to icing are still existent for small ships. Examples of the most recent documented icing incidents providing deceased, are from February 2007 at the east coast of the USA (United States Coast Guard, 2008), and from January

Figure 1: Ice mallet applied to remove ice during dangerous icing conditions on historical polar expeditions. The ice mallet is exhibited at the Polar Museum in Tromsø in Northern Norway. Photo: Eirik Mikal Samuelsen.

1999 at the coast of Northern Norway, costing the lives of 4 and 3 people, respectively. The latter is revealed by investigating the database of ship accidents from the Norwegian Maritime Authority (2014). In addition, there is also a recent accident that arose on 11 February in the present year outside Alaska. A crab-fishing vessel with a crew of six suddenly vanished north of an island called St. George in the Bering Sea. From the reports of other vessels this day it is believed that icing may have been the cause of a possible accident that led to capsizing, submerging, and the disappearance of the vessel (The Seattle Times, 2017). For larger ships the risk of capsizing is minimal. However, icing may lead to iced-down rescue equipment, ladders, handrails, and stairways (Løset *et al.*, 2006). Icicle build-up with a great risk of falling down may jeopardise the crew. For these reasons many ships operating in a cold climate, prevents ice from forming by using heat which is energy consuming. Thus, avoiding areas with icing is interesting also from a financial perspective (pers. comm. Kjell Are Berg-Hagen, Technical Director Tranberg AS, Member of the R. STAHL Technology Group, March 2017). Consequently, forecasts of icing are not only important to avoid fatalities, but a correct use of an accurate forecast when planning operations in Arctic seas may be economically advantageous for the ship companies. Alternatively to applying heat, one may hammer the ice lose with an ice mallet. This was the common method of removing ice in the earlier days (Figure 1)

1.2 Review of the evolution of ship-icing prediction methods

Marine-icing is an elusive process which has resulted in the fact that numerous studies and investigations have been carried out about this phenomenon during the last six decades. Consequently, only a short summary of the investigations most relevant for the focus of the current study is presented in the following section.

Due to several accidents with the loss of lives in the decades after the Second World War (Sawada, 1968; Shellard, 1974), closer attention is drawn to the phenomenon of ship icing in the 1960s. Icing is included in the synop code for ship observations (WMO, 1962), and several icing nomograms are established in this decade (Sawada, 1962; Mertins, 1968). These nomograms are based on empirical relationships between observations of icing and parameters like air temperature, sea-surface temperature, and wind speed for application in general weather forecasting. Such statistical forecasting methods, including the one generated from ship observations in the Baltic Sea in the 1970s (Lundqvist and Udin, 1977), are still applied in operational weather forecasting today (Paper III). Other studies in this period attempt to reveal relationships between icing and the synoptic weather situation based on upper-air parameters like the temperature at 850 hPa (Sawada 1967; Sawada 1968; Vasilyeva 1971; Borisenkov and Pchelko 1975). There is in general throughout these two decades a focus on the collection of icing data. This is particularly apparent in the literature of the former Soviet Union (e.g. Borisenkov and Panov (1972)). Since these observations have revealed that wave-ship interaction icing is the most frequent and dangerous cause of icing, this is also a starting point for the numerical prediction models of wave-ship interaction icing (Kachurin *et al.*, 1974). The model of Kachurin *et al.* (1974) is based on an empirical relationship between wave height and the liquid water content (l_{wc}) of the spray flux (R_w) based on spray measurements on a medium-sized fishing vessel (MFV) named Iceberg with a vessel speed of around 6 to 8 knots during the period of spraying ($l_{\mathrm{wc}} = 10^{-3} H_s$). Moreover, Kachurin *et al.* (1974) attempt to determine an icing rate (cm h^{-1}) on a cylinder by calculating several heat fluxes capable of freezing the sea water sprayed on this cylinder by wave-ship interactions. They find a rather extraordinary good fit ($r = 0.96 \pm 0.02$) between the observed ice-accumulation load rate (tonnes h^{-1}) on MFVs and calculated icing rates on the cylinder derived from the model. However, the reliability of the fit presented in Kachurin *et al.* (1974) has been doubted by Zakrzewski *et al.* (1988a), specifically since there are numerous uncertain parameters involved both in the model and observations utilised in the wave-ship interaction icing process. Stallabrass (1979a) is inspired by the model of Kachurin *et al.* (1974), but simplifies the number of terms involved in the model by only considering the heat fluxes from the atmosphere and the spray acting on the shipborne sea water sprayed on such a reference cylinder. He further develops the model by tuning the coefficient in the water-content term of the spray flux of Kachurin *et al.* (1974) to be in agreement with some icing-rate

measurements from 39 events collected at the east coast of Canada (Stallabrass, 1980) ($l_{wc} = 1.7 \times 10^{-4} H_s$). These measurements are weighted according to the location on the ship that these are recorded.

In the 1980s icing-rate data in conjunction with important input parameters in Alaska and the east coast of Canada are collected (Pease and Comiskey, 1985; Roebber and Mitten, 1987; Zakrzewski *et al.*, 1989). These three data sets are in the following abbreviated as P&C (Pease and Comiskey, 1985), R&M (Roebber and Mitten, 1987), and ZLH (Zakrzewski *et al.*, 1989). The P&C data set is applied as the basis to the development of the famous Overland predictor (Overland *et al.*, 1986) which is the most applied method for forecasting icing in operational weather forecasting today (Paper III). This model is also based on heat-flux calculations, but instead of calculating the spray flux from an empirically-based expression, the freezing fraction (n), i.e. the ratio between the icing and the spray flux, is held constant and adjusted in such a manner that fits best the observation of icing rates from Pease and Comiskey (1985). The model is further tuned by including some observations from a single ship type from ZLH in a later version of the model (Overland, 1990). Brown and Roebber (1985) incorporate a verification study of the methods of Mertins (1968); Kachurin *et al.* (1974); Stallabrass (1980), and a nomogram which are based on a method of Wise and Comiskey (1980). Brown and Roebber (1985) apply a selection of the data from Stallabrass (1980) and P&C. Roebber and Mitten (1987) also present a verification study of some methods applied in operational weather forecasting, namely Kachurin *et al.* (1974); Stallabrass (1980); Overland *et al.* (1986) and a simple statistical freezing index proposed by Brown and Roebber (1985). Roebber and Mitten (1987) applies both the P&C data and the R&M data, but conclude that the poor quality of the data sets, specifically the R&M data, is a major drawback of their evaluation.

In the same decade there is also a growing interest for marine icing due to increased oil and gas exploration in Arctic waters. According to Horjen (1990) his doctoral thesis is emerged from various icing projects connected to icing on offshore structures and supply vessels carried out during this decade. Horjen introduces a comprehensive mathematical model computing icing rates on idealised cylinders, and he specifically addresses a model for icing prediction on a vessel named "Endre Dyrøy" since there has been recorded both spray observations and icing observations from the same location on this vessel. Horjen and Carstens (1989) derive a spray-flux expression based on spray data from this vessel collected during a field campaign described in Horjen *et al.* (1986). The model is compared with ice-thickness measurements recorded at several locations of the front mast during two icing events lasting six and three hours, respectively (Horjen and Carstens, 1989). A major assumption in the spray-flux expression is that the relationship between wave height and wave period applies a fully-developed sea assumption following the Pierson-Moscowitz spectrum (Pierson and Moskowitz, 1964). A recent study by Horjen (2013) applies an updated version of his model,

and applies a relationship between both wind speed and wave height, and wave height and wave period, based on empirical relationships of these parameters from observations in the North Sea and a fishing bank outside Northern Norway called Tromsøflaket. Makkonen (1987) introduces the concept of spongy ice accretion in wet spray-icing models, i.e. that a fraction of water is encapsulated inside the icing matrix covered by a thin layer of brine. Sponginess is a phenomenon which is observed in both fresh and saline-water spray-icing events. A major assumption of Makkonen (1987) is that the so-called interfacial distribution coefficient (k^*) is independent of the environmental conditions, implying that the portion of brine water incorporated in the icing matrix is held constant. This leads to the fact that the brine salinity may be calculated from the freezing fraction derived in the heat equation. Horjen (1990) builds on this concept, and introduces a time dependency in the calculation of the properties of the brine film including brine salinity.

In the end of the 1980s Zakrzewski and co-authors present several studies focusing on the modelling of wave-ship-interaction icing for MFVs (Zakrzewski, 1986; Zakrzewski and Lozowski, 1987; Zakrzewski, 1987; Zakrzewski *et al.*, 1988a,b). In Zakrzewski (1987) empirical expressions for the time-averaged spray-flux of such a vessel are derived based on observations of spray-water content and duration time of sprays from MFV Narva (Borisenkov *et al.*, 1975), and spray frequency from a study of Panov (1971). Zakrzewski (1987) also addresses the application of an empirically-based relationship between wind speed and wave height, and wind speed and wave period, for fetch lengths in the ranges of 100-500 nautical miles. These formulas are derived from world-wide oceanographical data from various sources presented in a handbook of ocenographical tables (Bialek, 1966). In Zakrzewski *et al.* (1988b) the flight time and the velocity of the spray droplets are calculated by using an equation of motion and a mathematical expression for the perimeter of the ship viewed from above. Zakrzewski and Lozowski (1989) have translated and presented an overview of the main findings from the Soviet literature in the 1960s and 1970s including 115 observations of ice-load accumulation rate (tonnes h^{-1}) on such fishing vessels.

In the 1990s the model of Zakrzewski and Lozowski (1987) is further developed and adjusted towards a large US Coast Guard Cutter named Midgett, and icing is calculated on individual components over the entire ship (Zakrzewski *et al.*, 1993). The results of an expedition with this ship in which several parameters like spray-cloud duration time, spray frequency, and spray-water content are observed, are presented in Ryerson and Longo (1992) and Ryerson (1995). Finding an appropriate spray-flux expression when calculating icing for a different ship type seems to be the motivation for the work of Chung (1995) when applying the model of Zakrzewski *et al.* (1993) to calculate icing on the Stern trawler MT Zandberg. Chung (1995) and Chung *et al.* (1998) derive a spray-flux expression based on tank experiments by applying a small-scale model of the MT Zandberg and by scaling the environmental variables. Moreover, the icing model with this new

spray-flux expression is verified against the icing-rate observations of ZLH when these are converted to ice-load accumulation rate by multiplying the icing rate by the area of the foredeck, and the front and top of the wheelhouse, and an average ice density (Chung, 1995). Blackmore *et al.* (1994) and Blackmore (1996) on the other hand follow a different approach by calculating the heat balance between an assumed supercooled spray cloud and the surrounding air. Both the Chung (1995) and Blackmore (1996) approaches are tested against the Soviet icing data presented in Zakrzewski and Lozowski (1989). In the same period a modified version of the Stallabrass (1980)-model adjusted for application in operational weather forecasting is developed by Ross Brown (Henry, 1995) by including some of the findings of Zakrzewski (1986) for spray-cloud duration time and liquid water content of the spray.

After the introduction of the possibility of simulating the more complex three-dimensional structure of the ice accretion by applying a so-called morphogenetic modelling approach in Lozowski *et al.* (2000), there are only a few other studies about marine icing in the first decade after the year of 2000 (e.g. Forest *et al.* (2005)). However, there has been a resurrection of ship-icing and other marine-icing studies in the last 5 years (e.g. Hansen (2012); Horjen (2013); Kulyakhtin (2014); Jones and Claffey (2015); Hansen and Teigen (2015); Teigen *et al.* (2015); Horjen (2015); Dehghani *et al.* (2016a,b)). Probably some of this increased focus on the concept of marine icing in the recent years is due to the increased oil and gas activity in Arctic waters (Naseri, 2016). Some of these studies are introducing the concept of calculating the air flow by applying computational fluid dynamics (CFD) (Hansen, 2012; Kulyakhtin, 2014; Hansen and Teigen, 2015). Hansen (2012) applies observed ice-thickness measurements from the weather ship AMI recorded in the end of the 1970s. He extracted these icing data from the report of Eide (1983), while the other parameters used as input to the model are derived from the NOrwegian ReAnalysis 10 km data (NORA10). Kulyakhtin and Tsarau (2014) also apply NORA10 as a source of meteorological and oceanographical data for model input. However, they peculiarly derive the wave height from the modelled wind speed of the HIghResolution Limited Area Model (HIRLAM) applied in NORA10 at the location of interest instead of applying the modelled significant wave height based on the WAve Model (WAM) which utilises HIRLAM data. Teigen *et al.* (2015) calculate icing statistics in the Barents Sea based on the model of Hansen and Teigen (2015) by applying NORA10. However, these three studies do not discuss the quality of NORA10 when applied in icing modelling. Although some of these works are developed particularly for structures, some aspects regarding the icing process may potentially be applied in ship-icing modelling as well. Kulyakhtin (2014) and Kulyakhtin *et al.* (2016) particularly stress the importance of applying the conductive heat flux in pulsed spray-icing events based on experiments conducted with a nozzle of sea spray, sprayed under freezing conditions at light cylinders in Adventdalen in Svalbard. However, it is

questionable whether research conducted at light cylinders in weather conditions in a valley in Svalbard, are directly transferable to large surfaces in a wetter and more exposed environment on the superstructure of a ship operating in open ocean during wave-ship interactions (Paper II).

1.3 Research motivation, aims and scopes of the study

The thesis is a part of a project entitled: "Optimization of Ship Operations in Arctic Waters by Application of Sensor Technologies for Ice Detection, De-icing and Weather Data" and is related to a work package which deals with the development of a decision support system that can give the officer of a ship an early warning of the risk and growth-rate of icing (MAROFF, 2013). Although a decision support system may be based on the observed state of icing at different locations on a ship at present, it may also be developed by applying forecast of icing for days or weeks ahead in time for better planning of operations in a cold marine climate. The idea of supporting a particular ship with better icing forecasts is also of interest for the Norwegian Meteorological Institute which is a partner of the project. General ship-icing forecasts are generated twice a day by the Norwegian Meteorological Institute in the marine weather forecast for the High Seas (MET Norway, 2015) in the ice-free areas from 65 to 90 °N (Figure 2). A special warning is also issued when moderate or severe icing is expected in the coastal areas of Northern Norway. However, although such icing forecasts are regularly issued, usually based on

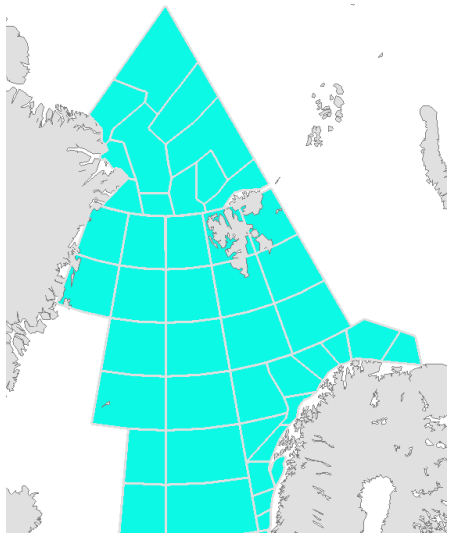

Figure 2: Areas included in the High Seas forecast generated twice a day from the Norwegian Meteorological Institute (MET Norway, 2015). A forecast is issued for each of the areas, in which some are fishing banks, separated in the figure by grey lines. Icing information is included in the forecast whenever an icing rate of moderate or severe icing is expected. Source: yr.no (2017b)

the methods of Overland (1990) or Mertins (1968), the quality of these forecasts has been little investigated. Furthermore, the issue that the icing-prediction methods apply different thresholds for moderate or severe icing is rarely challenged. In fact the threshold for an icing rate above moderate is 4 cm pr 24 h in the Mertins (1968)-method whereas it is above 0.7 cm pr hour in the Overland (1990)-model. In the recent years also the model named Modified Stallabrass has been applied at the Norwegian Meteorological Institute (Paper I; Paper III). Some of the reason for the lack of knowledge about the quality of the methods is indeed due to the fact that there are no ships at present regularly reporting icing in the Arctic-Norwegian waters. From the end of the 1970s until the beginning of the 2000s there were several ships manually recording icing in the ship-synop log book whenever it was encountered (Paper II). Nevertheless, in the last decade the observation recording system of the ships has been more automatised, and there are no longer any manually-collected recordings from e.g. the Norwegian coast guard ships.

Moreover, as highlighted in the previous section, in general throughout the years there has been sparse and little verification of the icing models, specifically in Arctic-Norwegian waters for the methods applied in operational weather forecasting. Previous verification studies have either used unreliable data with an insufficient number of parameters or data sets with very few data points in general, e.g. the advanced and time-dependent model of Horjen (1990) are only verified against data points recorded during two periods of icing. The complexity in the model is therefore not sufficiently justified by observations. In fact, for the Arctic-Norwegian sea areas the only icing data currently available is all the twelve events recorded on AMI described in Eide (1983), and the two periods of icing listed in Horjen and Carstens (1989). Consequently one of the main goals of this study is to find more accurate icing data in conjunction with necessary input parameters from these sea areas. If this is fulfilled the quality of the current methods applied in operational forecasting may be evaluated. According to Makkonen *et al.* (1991) there are for instance reasons to believe that the Overland (1990)-model is overestimating icing in areas with low sea-surface temperatures. As a matter of fact, predictions of severe icing near the ice edge in which low SSTs occur are particularly apparent when applying numerical prediction models as input to the Overland model (Figure 3). In many cases other methods do not indicate such severe conditions near the ice edge as indicated by the Overland model as illustrated in Figure 3.

It is also manifested that the uncertainty regarding the necessary meteorological and oceanographic parameters applied as input to the icing models in many aspects have been neglected in previous studies. Thus, inaccurate icing predictions have often been addressed only to the inaccuracies in the physical considerations of the spray- and icing-modelling part. Neither the uncertainty regarding the application of empirically-based relationships between wind and wave parameters for wave-parameter estimations has been addressed, nor the application of NORA10

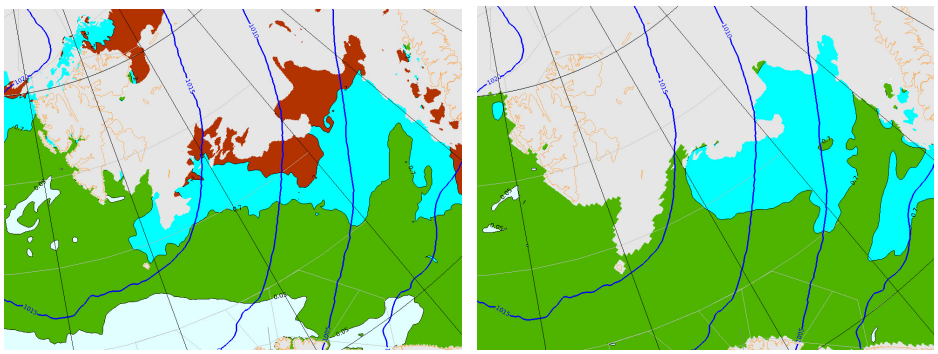

(a) **(b)**

Figure 3: Example of light (green), moderate (cyan), and severe (red) icing predictions from a) the Overland model (Overland, 1990), and b) the original Modified Stallabrass model applying the definition of icing rates from Overland *et al.* (1986) (Paper I; Paper III). The version of these models in the figures are the ones described in Paper I as the model O1 and M1. The figure shows a 12-hour forecast of icing from 24 March 2015 for the sea areas between Northern Norway and Svalbard. The HIRLAM model with 8 km horizontal resolution is applied as input to the icing models, and for the Modified Stallbrass model the significant wave height applied as input to the model is derived from the WAM model with 10 km horizontal resolution. The grey areas represent the areas where the model input data are not defined either due to land or sea-ice cover. Since the WAM model applies cruder sea-ice information than does the HIRLAM model, there are some differences regarding the areas with defined icing rates in the two methods near the ice edge. Blue lines describe mean-sea-level pressure (MSLP) with a contour spacing of 5 hPa.

data in conjunction with icing predictions (Paper II). Another goal of the study is therefore to check if these assumptions are valid, and evaluate whether such assumptions when applied in an icing model degrade icing-rate predictions.

A part of the evaluation of icing models and observations, is also to investigate which parameters are most important during icing events. Are there any additional parameters important for icing that have not been addressed in earlier studies? An extension to this is to consider in which kind of weather situations icing ensues in these sea areas. It is of particular interest to check whether freezing rain, fog, or snow events play an important role in ship-icing events.

Finally, the ultimate goal is to develop a prediction method based on numerical prediction models of the atmosphere and the ocean that may be applied in operational weather forecasting in order to provide the officer on ships operating in the actual waters an early warning about the icing risk. Thus, evaluation of short-term icing predictions of a couple of days is of interest, but also evaluation of the potential of finding methods for predictions exceeding a couple of days or even a week are relevant. If such warnings are issued on a map like Figure 3, it may be possible for the officer of a ship to adjust his or her route and avoid areas of icing according to the icing predictions. For long-term icing predictions he or she may

also postpone a certain voyage if there is a high risk of icing in the prognoses.

The research questions, aims, and scopes may be summarised as follows:

- R1 Collect applicable icing data with necessary input parameters in Arctic-Norwegian waters.
- R2 Evaluate the quality of existing methods applied in operational weather forecasting.
- R3 Evaluate the importance of the uncertainty of the input parameters used in icing models for icing predictions.
- R4 Investigate which weather parameters are most important, and which weather situations occur most frequently during icing events.
- R5 Develop a short-term and long-term prediction method for icing with higher accuracy than previous methods applied in operational weather forecasting.

2 Methodology

2.1 Icing-data collection

When delving into the topic of marine icing, there are many circumstances that are more convoluted than one may initially anticipate. For these reasons it is important to define the constrictions relevant to the part of the icing problem investigated. For this study the main focus is on the development of a general forecast of the severity of icing based on input parameters from a particular state of the atmosphere or the ocean at a future time step presented on a map. This is different from a calculation of a total ice load on a ship following a specific route. For the latter approach the temporal variation in the state of the atmosphere, ocean, and ship movement is more crucial, both when these are obtained from observations and numerical prediction models. Accounting for issues regarding the melting of ice and mechanical ice break-off may also be necessary. When evaluating total ice-load accumulation data during a particular trip plenty of details regarding the local variability in ice thickness and ice density are important to consider in order to estimate such ice loads accurately. At present most of such data are non-existent and may be time consuming and resource demanding to collect, both from a financial and a human perspective. It is also questionable to model ice loads without an estimation of the highly irregular wind pattern around the ship which among other things control the areas exposed to sea spray. This is one of the reasons why only those ships with an angle between the wind and ship (β) between 90 and 180 $^\circ$ are selected in the data collection process for ice-accumulation data in the present study. Sea spray may namely be encountered in the aft of the ship in a turbulent air flow although the wind and ship are headed in opposite directions (Kulyakhtin *et al.*, 2012). Furthermore, such wind patterns may be interrupted by convective plumes and snow showers when cold winds blow over relatively warm waters (Paper II). According to Makkonen and Fujii (1993) icicle build-up and correct icicle spacing must also be included in ice-load models in order to achieve accurate ice-load predictions.

For these reasons it is determined at an early stage of this project to utilise the existing icing data from the ship-synop registrations in order to generate icing-rate information based on ice-thickness differences from a particular location on the ship. The icing and sea-ice information recorded in the ship synop are described in Figure 4. The icing information is included in group 22 starting with the number 6 following four digits with information recorded in three columns. The first column (I_S) is a code for the cause of icing[1]. The next column including two digits is the total ice accumulation reported in whole centimetres (E_S). The last column is a subjective estimate of ice accretion at the time of the observation (R_S)[2]. There

[1] I_S = 1: pure spray, 2: pure fog, 3: fog and spray, 4: freezing rain, 5: freezing rain and spray.

[2] R_S = 0: ice not building up, 1: ice building up slowly, 2: ice building up rapidly, 3: ice melting or breaking up slowly, 4: ice melting or breaking up rapidly.

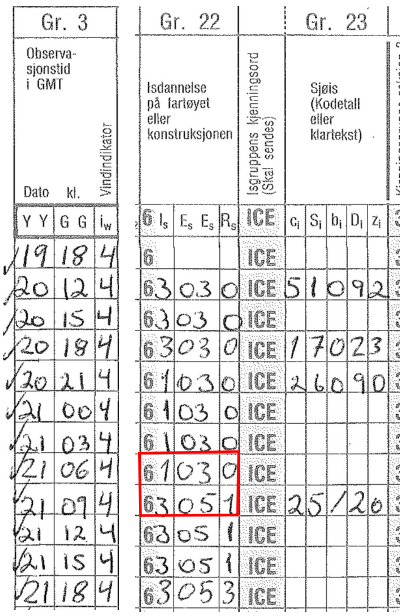

Gr. 3				Gr. 22					Gr. 23				
Observasjonstid i GMT			Vindindikator	Isdannelse på fartøyet eller konstruksjonen				Isgruppens kjennetegnord (Skal sendes)	Sjøis (Kodetall eller klartekst)				
Dato		kl.											
Y Y	G G		i_w	6 I_s	E_s	E_s	R_s	ICE	c_i	S_i	b_i	D_i	z_i
19	18		4	6				ICE					
20	12		4	6	3	0	3	ICE	5	1	0	9	2
20	15		4	6	3	0	3	ICE					
20	18		4	6	3	0	3	ICE	1	7	0	2	3
20	21		4	6	1	0	3	ICE	2	6	0	9	0
21	00		4	6	1	0	3	ICE					
21	03		4	6	1	0	3	ICE					
21	06		4	6	1	0	3	ICE					
21	09		4	6	3	0	5	ICE	2	5	1	2	0
21	12		4	6	3	0	5	ICE					
21	15		4	6	3	0	5	ICE					
21	18		4	6	3	0	5	ICE					

Figure 4: Example of icing and sea ice measurement from the handwritten ship synop code recorded on KV Andenes in the period 19 to 21 January 1987. The ship is travelling southwards from Svalbard to Northern Norway. From 21st January 0600 UTC to 0900 UTC there is an increase in ice thickness from 3 to 5 cm (E_S) marked with a red square. In this event there is 2 cm ice accumulation in 3 hours (0.67 cm h^{-1}). The cause of icing is pure sea spray (I_S = 1) at 0600 UTC and sea-spray and fog (I_S = 3) at 0900 UTC. According to the subjective estimate of ice accumulation, there is a gradual increase in icing at 0900 UTC (R_S = 1) and no ice-accumulation at 0600 UTC (R_S = 0).

are 17 ships that has reported icing in these sea areas from the end of the 1970s to the beginning of the 2000s. However, for most of these ships, it is not clear at which location on the ship the icing information is recorded. Fortunately, for the KV Nordkapp ship class, it is discovered that the icing observations are recorded at a specific position on the ship according to an interview with a former marine officer serving these ships in the 1980s and the 1990s (Paper I). Consequently, it is determined to specifically focus on applying the ice-accumulation data from the KV Nordkapp ships (KV Andenes, KV Nordkapp, and KV Senja) for icing-rate verification purposes. Moreover, the Norwegian Coast Guard allowed publication of their historical data although this information is originally regarded as restricted for the public (Paper I). As an additional quality-check of the ship data, the handwritten ship-synop observations are compared to the electronically stored ones (Figure 4), and some errors in the data stored in the electronic database at the Norwegian Meteorological Institute are corrected. Unfortunately the handwritten recordings were only available in the years 1986 to 1995 at the Forecasting Division Western Norway (Paper II). Hence, there are some minor inaccuracies

particularly regarding the relative humidity data in the data utilised from the years outside this interval.

Regarding icing-data utilisation the four papers use the following icing information: Paper I applies ice-thickness data (converted to icing rate) recorded in a particularly well-documented severe-icing voyage during a developing polar low in the Barents Sea with observations recorded every three hours. In Paper II more comprehensive screening and quality-checks are performed on all of the KV Nordkapp ship data, and icing information is collected only for those ships with an angle between the wind and ship in the range from 90 ° to 180 °, and with a start position of the trip not located in packed sea ice ($C_I < 0.4$ or not reported). Only those observations are applied with a time difference less than or equal to nine hours between two consecutive junctures with an increase in the ice thickness between these junctures. Paper III applies the data of Paper II, and applies data from the P&C and R&M data where reanalysis data from various sources have been supplemented in the data sets for missing or uncertain parameters. For the P&C data only those events having $\beta \in \langle 90, 180]^\circ$ and enduring shorter or equal to 12 h are applied. For the R&M data only those events with the necessary ship and position data are applied. Temperature data in this data set is replaced with ERA-Interim temperatures (Dee *et al.*, 2011). Hence, only events with negative ERA-Interim temperatures are selected. Paper IV follows a different procedure utilising the subjective icing-rate information (R_S) in order to discriminate events with icing from no icing, and compare these with atmosphere and ocean variables recorded at the same junctures as the icing information.

2.2 Application of parameters in conjunction with icing information

An advantage of applying ship-synop data for icing is that such data also incorporates information about several other parameters in which many are important for icing-rate calculations. The following parameters are included in a standard observation sheet for the Norwegian Coast Guard:
Time, position, total cloud cover (N_N), cloud height of lowermost cloud, visibility, wind direction and speed, air temperature (T_a), relative humidity (R_H), dew-point temperature derived from T_a and R_H, mean-sea-level pressure (MSLP), change in pressure last 3 hours, present weather at observations time (W_W), past weather occurred since the main observation time at 0000, 0600, 1200 or 1800 UTC, cloud types of low-, medium-, and high-level clouds including cloud amount of low- or medium-level clouds, sea-surface temperature (SST), wind-wave height, wind-wave period, swell-wave height, swell-wave period and swell-wave direction, icing information, and sea-ice information. A crude estimation of the speed and the course during the last three hours are sometimes included, but it is determined to apply the position data for speed and course calculation since this information seemed to provide more accurate directions and speeds during the travel be-

tween the two junctures considered. Position data are also included more regularly than the speed and course estimation. Since the wave information is visually estimated a correction method is applied from the basis of a paper of Gulev and Hasse (1998) which compared such ship observations with buoy data in the Atlantic ocean. Details are provided in the Appendix A of Paper II. However, salinity data, bathymetry data, radiation data, and precipitation data are not observed on the ship. The two latter are collected from NORA10, and the two former are collected from Nordic Seas 4 km numerical ocean model hindcast archive (SVIM) (Lien *et al.*, 2013). Bathymetry data are not utilised in former icing studies, since deep-water approximation is always applied for wave-phase speed and wave-group speed calculations. However, such data are collected to check whether deep-water approximation is a valid approach in icing events. For sea-surface temperature the observed values, the SVIM values, and the NORA10 values are all compared with each other. It is concluded that the observed SST and SVIM SST have the smallest difference in most instances (Paper II), and SST values from these two sources are therefore considered the most reliable ones.

Early in the research process it was also a question whether reanalysis data are applicable at all for icing-rate calculation purposes. This was a particular concern after comparing NORA10 during the polar low case in Paper I with observations (Section 3.1). In this particular event, there is an underestimation of the wind speed of 9.6 m s^{-1} and an overestimation of the temperature of 3.8 °C in NORA10. However, after testing NORA10 applied as input to MINCOG and compared the results with the modelled icing rate with the use of observations, it is concluded that applying NORA10 does not considerably worsen the icing rate predictions for all the KVN events despite the fact that there still is an underestimation of wind speed of 4.2 m s^{-1} and overestimation of temperature of 2.2 °C for these events (Table 2 in Paper II).

Due to the thorough screening, meticulous selection process, and inclusion of most parameters relevant for icing-rate calculations, the 37 icing events of a single ship type presented in Paper II are regarded as unique. In addition, several events with no accumulation from the same ship type are also considered (41 in Paper II, which are reduced to 30 in Paper III). For comparison with other ship-icing events, the icing events of P&C and R&M are included in the analysis in Paper III. For these data sets, reanalysis data from ERA-Interim, Wavewatch III (Tolman, 2014), NOAA High resolution SST (for the R&M data), and average annual climatology values of salinity (National Oceanographic Data Center World Ocean Atlas 1994 by NOAA) are all applied (Paper III). These sources of reanalysis data have courser horizontal resolution than the reanalysis data applied in the KVN data set. The exact hour that the events in the P&C and R&M data arose is also uncertain, hence the daily average values of the reanalysis parameters are applied. Thus, the temporal resolution of the supplemented reanalysis data in the P&C and R&M data is lower than the reanalysis data used in the KVN data.

The ship observations are only providing information about the atmospheric conditions near the surface. On the other hand, Paper IV utilises upper-air data to extract information about the weather situation during icing. Data from the 40 models levels of NORA10 are applied in order to evaluate the weather situation occurring in 333 icing and 468 no-icing events from 17 different ships operating in the Barents Sea, the Greenland Sea, and the Norwegian Sea from 1980 to 2006. Map composites and vertical cross sections are generated to illustrate the average weather in these events.

2.3 Model development

As described in Section 1.2, there has throughout the years been different approaches regarding modelling of marine icing. Although the major driving force is apparently prediction, some studies are focusing on understanding the processes involved, while others are more developed for direct application in marine weather forecasts. Others again are more specified towards forecasting total ice thickness or ice loads for a particular ship following a particular route. However, there has in the past been little discussion about the time frame of icing forecasts, and their validity for long-term predictions. Obviously advanced modelling approaches involving many parameters are more uncertain for forecasts with longer time spans (Paper IV). During the last 60 years of icing research there also seems to have been a change from the crude statistical modelling approaches applied in the first studies to a more detailed wave-ship-interaction icing-modelling approach with a process of progressively adding more complexity into the models. The initial thought in the current study was to follow the pathway of the wave-ship interaction modelling approach and adding the parameters or considerations that seemed most crucial to include. However, it was soon discovered that it was not easy to judge whether an initial term or consideration was justifiable, particularly since there are inaccuracies in the utilised icing-rate data (ice-thickness recordings measured with a ruler). As a consequence, it was not easy to state whether more complexity, although being more physically reasonable, would increase the quality of the prediction. This is specifically important to bear in mind when considering the fact that the input of the model ought to be forecast parameters from the atmosphere and ocean with lead times up to a couple of days.

2.3.1 Spray-flux calculation

The MINCOG model is developed on the basis of an empirical time-averaged spray-flux expression, developed for an estimation of the spray flux at the horizontal mid-point of the plate where icing is encountered on KV Nordkapp ships. The spray flux is tuned for the height above sea level where icing arose, and with droplet velocity calculated from a mathematical droplet trajectory model apply-

ing an expression for the gunwale of the KV Nordkapp ship. Spray frequency and spray-cloud duration times are adjusted towards this larger ship type. Two data sets of sea spray have been utilised in the model, where one of those based on spray data from Horjen *et al.* (1986) (Horjen spray-flux expression) has been updated with more accurate meteorological data obtaining a better fit than the one applied in Horjen (2013) (Paper II). However, the spray-flux expression based on the spray data of Borisenkov *et al.* (1975) (Borisenkov spray-flux expression) encountered highest verification scores when applied in MINCOG, and is therefore applied in later evaluations (Paper III). This latter expression may be formulated as follows:

$$R_w = \mathbf{V_d} \cdot \mathbf{n_1} l_{\mathrm{wc}} N t_{\mathrm{dur}} \tag{1}$$

where

$$\mathbf{n_1} = [\sin\gamma, 0, \cos\gamma], \quad \gamma = 85^\circ \tag{2}$$

$$l_{\mathrm{wc}} = 6.36 \times 10^{-5} H_s V_r^2 \exp\left(-0.55\,(z-3.5)\right), \quad z \in [6.5, 8.5]\ \mathrm{m} \tag{3}$$

$\mathbf{V_d}$ is the three-dimensional droplet velocity or spray velocity at impact towards the plate in consideration with a tilt angle (γ) relative to the horizontal in a coordinate system following the ship (Figs.2 and 3 in Paper II), $\mathbf{n_1}$ is the normal vector of this tilting plate (Eq. (2)), l_{wc} is the liquid water content of the spray adopted from Zakrzewski (1987), but with a slightly adjusted constant (Eq. (3)), N is the spray frequency, and t_{dur} is the residence time of the spray cloud. More details are presented in Paper II. In Paper I, one of the test models (T3) applies a different formulation for the liquid-water content of the spray adopted from Roebber and Mitten (1987). For this reason it was desirable to also evaluate the MINCOG model in Paper III with a formulation that incorporates the physics of this method. It is then assumed that l_{wc} is a function of the wave energy flux ($\propto H_s^2$), the square root of wave steepness ($(H_s/\lambda)^{0.5}$) and the wave group velocity. However, the relative velocity between the ship and the wave groups seems to be a more appropriate variable to apply instead of the absolute wave group velocity applied in Roebber and Mitten (1987). This new l_{wc} can then be written as follows:

$$l_{\mathrm{wc}} = w_0 H_s^2 \left(\frac{H_s}{\lambda}\right)^{0.5} V_{\mathrm{gr}} \exp\left(-0.55(z-3.5)\right) \tag{4}$$

where

$w_0 = 9.5205 \times 10^{-4}\ \mathrm{kg\ s\ m^{-6}}$

$z \in [6.5, 8.5]\ \mathrm{m}$

The constant w_0 is adjusted from the weather information in Borisenkov *et al.* (1975) as in the method of Zakrzewski (1987). However, a wave height of 4.25 m is applied instead of the wind-speed derived value of 3.19 m from Zakrzewski (1987). This is the mean value between 2.5 and 6 m (sea state 5 and 6), which was

the reported sea state during the excursion in the original reference (Borisenkov *et al.*, 1975). The verification scores of a MINCOG model which incorporates this formulation are presented in the results section of the thesis, since it had to be left out of Paper III in order to reduce the number of models and variations of models evaluated in that paper. This model is entitled MINCOG adj (Section 3.3).

2.3.2 Heat-flux calculation

A heat balance is calculated from the heat fluxes acting on the estimated R_w in the position at the horizontal mid-point of the almost vertical plate ($\gamma = 85\ ^\circ$). The full set of heat fluxes pr unit area acting on this plate may be written as:

$$Q_f = -Q_v - Q_k + Q_c + Q_e + Q_r + Q_d + Q_s + Q_{\text{cond}} \tag{5}$$

The fluxes on the right hand side of Eq. (5) are arranged in such a manner that they contribute to freezing if they are positive, and negative if they contribute to melting. These fluxes will then balance the heat released due to freezing (Q_f) on the left-hand side of Eq. (5). A short explanation of these fluxes is as follows:

Q_f	-	Latent heat released during freezing
Q_v	-	Viscous/frictional/aerodynamic heating from the air
Q_k	-	Kinetic energy of spray converted to heat in the interaction process
Q_c	-	Convective or sensible heat flux from the air
Q_e	-	Evaporative or latent heat flux from the air
Q_r	-	Heating or cooling from radiation ($\downarrow\uparrow$ LW, $\downarrow\uparrow$ SW)
Q_d	-	Heating or cooling from the spray
Q_s	-	Heating or cooling from snow
Q_{cond}	-	The conductive heat flux through the ice

A further elaboration of these fluxes and their importance in the icing calculations in the current study are presented in the following sections.

2.3.3 Viscous heating from the air flow (Q_v)

Viscous heating of the brine from the air stream may be given as (Makkonen, 1984b):

$$Q_v = h_a r_a \frac{W_r^2}{2c_p} \tag{6}$$

This is a heating term which may contribute to melting. Since the ship is moving, the relative wind speed (W_r) is applied instead of the absolute wind speed. This term is usually neglected in marine-icing modelling. When applying values from

the KVN data set presented in Paper II, and using these as input to the MINCOG model with the Borisenkov spray-flux expression (Eq. (1))[3], this term will provide a maximum value of 55.7 W m^{-2}, and in the mean 9.0 W m^{-2}. For the extreme case this value is in fact in the same range as the calculated mean value of the Q_r from Table 3 in Paper II ($\sim$ 60 W m^{-2}). However, the mean value is approximately one order of magnitude lower than the extreme value, and neglecting this term seems for most of the events to be a reasonable assumption.

2.3.4 Kinetic energy of spray (Q_k)

Kinetic energy of the spray may be given as (Lozowski *et al.*, 1983):

$$Q_k = 0.5 R_w V_d^2 \tag{7}$$

This energy is converted into heat, and consequently contributes to melting. This term is also usually neglected in marine-icing modelling. If applying maximum and mean values for R_w and V_d, as for the Q_v-term[4], this flux has a maximum value of 27.2 W m^{-2}, and is in the mean 2.2 W m^{-2}. These values are even smaller than the values of the Q_v-term, and much smaller than the values of the prevailing fluxes of several hundreds W m^{-2} (Table 3 in Paper II).

2.3.5 Convective and evaporative heat flux (Q_c, Q_e)

The convective and evaporative heat fluxes are the two dominating terms in the right hand side of the heat balance equation (Eq. (5)). These terms may be expressed as e.g. (Paper II):

$$Q_c = h_a(T_s - T_a) \tag{8}$$

$$\begin{aligned} Q_e &= h_e(e_s(T_s) - R_H e_s(T_a)) \\ &= \frac{1738.6}{p} h_a(e_s(T_s) - R_H e_s(T_a)) \end{aligned} \tag{9}$$

It is assumed that the surface temperature of the brine (T_s) is equal to the freezing temperature calculated from the brine salinity (S_b). Based on the work of Makkonen (1987, 2010) it is then assumed that the brine salinity is determined only from the freezing fraction in spongy spray ice when the sponginess factor (interfacial distribution coefficient) is set equal to 30 % ($k^* = 0.3$):

$$S_b = \frac{S_w}{1 - 0.7n} \tag{10}$$

[3] $\max(h_a)$ = 86.0 W m^{-2} °C^{-1}, $\max(W_r)$ = 37.0 m s^{-1}, $\bar{h_a}$ = 52.6 W m^{-2} °C^{-1}, $\bar{W_r}$ = 19.6 m s^{-1}, r_a = 0.95 is a recovery factor for a vertical plate according to Horjen (1990)

[4] $\max(R_w)$ = 112.1$\times$ 10^{-3} kg m^{-2} s^{-1}, $\max(V_d)$ = 26.9 m s^{-1}, $\bar{R_w}$ = 15.1$\times$ 10^{-3} kg m^{-2} s^{-1}, $\bar{V_d}$ = 17.0 m s^{-1}.

Temperature changes of the brine surface with time due to changes in brine salinity with time due to salt expulsion, as is stressed to consider according to Kulyakhtin *et al.* (2016), are neglected. Brine salinity is only determined by the freezing fraction (n) which depends on the overall heat flux calculation. If neglecting the vertical wind and ship movement, the heat-transfer coefficient (h_a) may be decomposed in a horizontal component parallel to a vertical plate and another horizontal component normal to a vertical plate. The total heat-transfer coefficient are then written as some weight of these two components according to the weight of the components of the relative wind speed (Paper II):

$$h_{\mathrm{ay}} = 4.85 \left| W_{\mathrm{ry}} \right|^{0.8} \tag{11}$$

$$h_{\mathrm{ax}} = 6.06 \left| W_{\mathrm{rx}} \right|^{0.82} \tag{12}$$

$$h_a = w_1 h_{\mathrm{ax}} + w_2 h_{\mathrm{ay}} \tag{13}$$

The along-flow component is obtained from laboratory experiments for a flat plate with a characteristic length (D) in a turbulent air flow (Rohsenow and Choi, 1961), and the cross-flow component is obtained from CFD simulations for the heat exchange between the atmosphere and houses simulated as cubes with 10 m sides (Defraeye *et al.*, 2010). The two expressions are here adjusted for the width (D = 4 m) of the almost vertical wall of KV Nordkapp. For the calculation of the Q_e, the saturation-vapour pressure of Bolton (1980) is applied. For the ranges of the observed values of the icing events in the KVN data set, the fourth degree polynomial fit of Stallabrass (1980) may also be applied. However, applying the linearised version of Kulyakhtin and Tsarau (2014) is not recommended since it provides unrealistically low saturation-vapour-pressure values (even negative values) for the lowermost air temperatures in the ranges of the observations from the KVN data set (Figure 5). The salinity effect on the saturation-vapour pressure of the brine surface is also neglected (Paper II).

2.3.6 Radiative heat flux ($\mathbf{Q_r}$)

In contrast to other marine-icing studies (e.g. Horjen (1990); Lozowski *et al.* (2000)) the Q_r-term incorporated in this study includes both longwave and shortwave radiation (Paper II). Shortwave radiation has particularly some notable effect in the end of the winter season when there is daylight 24-hours a day at high latitudes. However, for simplicity only diffuse radiation is considered, since direct sun-light radiation absorbed on the vertical plate will be very sensitive to the position of the ship relative to the sun and fractional cloud cover due to the low sun angles in such events. Although the application of diffuse radiation alone is not a reasonable assumption in clear-sky conditions in April or May, Paper IV illustrates that most icing events also occur in cloudy conditions. In fact, more than 75 % of 429 icing events observed in Arctic-Norwegian waters between 1980 and

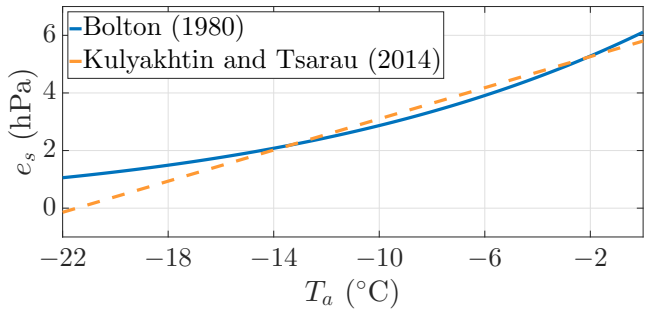

Figure 5: Sensitivity test of the saturation-vapour pressure of the expression from Bolton (1980) ($e_s = 6.112\exp\left(\frac{17.67T_a}{T_a+243.5)}\right)$ hPa) and the linearised version of Kulyakhtin and Tsarau (2014) ($e_s = (-6803 + 27.03(T_a + 273.15))10^{-2}$ hPa) relative to the approximate range of the observed temperature values in the KVN data ($T_a \in [-21.2, -1.4]$ °C).

2006 have an observed total cloud cover of six oktas or more (Figure 3 Paper IV). Longwave radation is derived from reanalysis data in order to take into account a more realistic emissivity of the atmosphere due to among other things the vertical change of temperature and humidity in the lowest layers of the atmosphere. Specifically when the temperature and humidity are rapidly dropping with height, as is often the case in the icing events ensuing from cold-air outbreaks, the longwave radiation from the atmosphere would be lower than that calculated from the 2 m or ship-observed temperature alone which is normally applied in other marine-icing models (e.g. Horjen (1990); Lozowski *et al.* (2000)). The radiative heat flux is therefore expressed as follows:

$$\begin{aligned} Q_r &= \uparrow \mathrm{LW} - \downarrow \mathrm{LW} + \uparrow \mathrm{SW} - \downarrow \mathrm{SW} \\ &= \sigma(T_s + 273.15)^4 - \downarrow \mathrm{LW} - (1-A) \downarrow \mathrm{SW} \end{aligned} \tag{14}$$

A view factor ($V_f = 0.5(1+\cos\gamma)$) is applied when converting the incoming shortwave radiation ($\downarrow$ SW) towards a horizontal surface provided by reanalysis data to the plate with a tilt of γ = 85 ° relative to the horizontal (Fig.2 in Paper II). In Paper II and Paper III the longwave radiation from the sea or the ship is not considered, but this may for instance be added to the incoming longwave radiation by introducing a weighting of these terms in the following form:

$$\downarrow \mathrm{LW} = 0.5 \downarrow \mathrm{LW}_{\mathrm{atm}} + 0.25\sigma(\mathrm{SST} + 273.15)^4 + 0.25\sigma(T_a + 273.15)^4 \tag{15}$$

It is then assumed that the longwave radition of the atmosphere towards a horizontal surface ($\downarrow \mathrm{LW}_{\mathrm{atm}}$) contributes to half of the total $\downarrow$ LW on an almost vertical plate, and that the rest is longwave radiation from the sea and components on the ship. It is then assumed that approximately half of this rest contribution comes from surfaces with temperatures equal to the sea-surface temperature and half of

the contribution comes from surfaces with temperatures equal to the air temperature. On the ship there may be wetted surfaces which have temperatures in the range between these two values, so both expressions include radiation which may stem from the surfaces on the ship.

2.3.7 Heat flux from the spray (Q_d)

A general form of the heat flux from the spray or spray droplets (Q_d) may be written as (Henry, 1995):

$$Q_{\mathrm{d}} = R_w c_w (T_s - T_{\mathrm{sp}}) f \quad \text{where} \quad f = n(1 - a_{\mathrm{ro}}) + a_{\mathrm{ro}} \tag{16}$$

The MINCOG model in Paper II and Paper III applies a run-off parameter equal to one (a_{ro} = 1), which is the assumption that all of the heat from the time-averaged spray flux is cooled down to the brine-surface temperature and is contributing in the thermodynamics. Hence, possible run-off water or splash water leaving the surface with less heating or cooling of the brine surface is neglected. The Q_{d}-expression with an a_{ro}-parameter different from one follows the argumentation from Kachurin *et al.* (1974) that only the part of the time-averaged spray flux that actually freezes are fully cooled down to the surface temperature (T_s), and that the rest of the water are only cooled down to a certain run-off temperature (T_{ro}). In fact, it may be shown that Eq. (16) may be written as:

$$Q_{\mathrm{d}} = nR_w c_w (T_s - T_{\mathrm{sp}}) + (1-n) R_w c_w (T_{\mathrm{ro}} - T_{\mathrm{sp}}) \quad \text{where} \quad (T_{\mathrm{ro}} - T_{\mathrm{sp}}) = a_{\mathrm{ro}} (T_s - T_{\mathrm{sp}}) \tag{17}$$

It is therefore apparent that the a_{ro}-parameter determines the fraction of the temperature difference between the surface and the spray that yields the temperature difference between the run off and the spray. The a_{ro}-parameter is set equal to 0.25 in Henry (1995) following the values obtained from laboratory experiments according to Kachurin *et al.* (1974). This implies that for freezing fractions close to zero, just a little more than 25% of the incoming spray flux will fully contribute to the heat flux term of the spray following Eq (16). For a freezing fraction equal to one, all of the incoming spray will contribute to this heat flux. In fact, the overall effect of adding such a run-off term, is similar to reducing the effect of the spray flux in the thermodynamics as is done in the time-dependent models of Horjen (1990) and Kulyakhtin (2014). In these models the Q_d-term is only involved during the period of spraying, and not in the periods between spraying. As a consequence, the time-dependent models are less sensitive to the sea-surface temperature than the models applying continuous spray flux without run off (Ekeberg,

2010). However, when applying such time-dependent calculations it is assumed that the duration time of the spray events and the frequency of the spray events are regular and well-defined quantities. This is probably questionable assumptions. A model including the a_{ro}-parameter equal to 0.25 was initially added to the analysis in Paper III, but was later removed. Thus, in order to complete the analysis, the verification results of this model is presented here in the results section (MINCOG adj ro) along with the results from applying the alternative spray-flux formulation without run off (MINCOG adj).

It is also worth noticing that the spray temperature (T_{sp}) is set to an intermediate value between a calculated droplet temperature (T_d) and the sea-surface temperature (SST). The spray cloud consists namely of a combination of single droplets which may lose considerable heat to the atmosphere during their flight and of more dense consolidations of droplets with less heat loss to the atmosphere. Droplet-temperature calculation is described in more detail in Paper II.

2.3.8 Heat flux from snow ($\mathbf{Q_s}$)

Due to challenges regarding obtaining accurate information about snow amounts, a model which includes snow as a contributing factor to icing is not included in the analysis of Paper I, Paper II, or Paper III. Horjen (1990) on the other hand includes snow in the marine-icing model by the application of the formula of Stallabrass (1979b) relating the water-equivalent snow amount to the observed visibility during snow falls. However, since both visibility and snow amount are highly irregular variables during snow showers in general, and particularly in these sea areas with the possible developments of polar lows during icing (Paper I), it is not possible to apply the observed visibility at two junctures to represent the average visibility or snow amount during the whole event. In addition, due to the variations in "crystal types, degree of riming, degree of aggreation, degrees of crystal wetness", and differences between visually-estimated visibility values of day and night, there is in most cases not a unique relationship between snow fall and visibility (Rasmussen *et al.*, 1999). Precipitation amount from NORA10 is presented in Paper II for the KVN data, but the accuracy of this data is unknown. In general, it is hard to measure solid precipitation in windy conditions as in the offshore icing conditions. It is for instance not clear how such solid precipitation sticks to a wetted brine vertical surface. Anyhow the snow amount that sticks to a vertical surface will probably be different than what is measured in a rain gauge with the opening in the horizontal plane which has low catch ratios for high wind speeds (Rasmussen *et al.*, 2012).

Despite these uncertainties a possible estimate of the water flux from the snow

may still be provided (Nygaard *et al.*, 2013):

$$\begin{aligned} R_{\text{snow}} &= l_{\text{wcsnow}} \mathbf{V_{snow}} \cdot \mathbf{n_1} \\ &= \frac{P_P}{V_t} \mathbf{V_{snow}} \cdot \mathbf{n_1} \\ &= \frac{R_R}{\Delta t V_t} \mathbf{V}_{\text{snow}} \cdot \mathbf{n_1} \end{aligned} \tag{18}$$

R_R is the accumulated precipitation amount during the duration of the event (Δt), and P_P is the precipitation intensity. $\mathbf{V_{snow}}$ is the velocity of the snow flakes assumed to be equal to the relative wind velocity in the horizontal direction and the terminal velocity of snow flakes (V_t) in the vertical direction. V_t may be set to e.g. 1.7 m s^{-1} (Nygaard *et al.*, 2013). The heat flux from the snow may then be calculated according to:

$$Q_{\text{s}} = R_{\text{snow}} c_s (T_s - T_a) \tag{19}$$

It is here assumed that all the snow is accumulated by the brine water, and the possible pulsating effect of collecting snow flakes in periods of showers is fully neglected. However, it is important to determine how much snow may be accumulated by the brine surface before the brine-snow substance is saturated with snow in which subsequent snow bounces off or blows away. It is also a challenge to determine the resulting brine salinity and density of the resulting ice. A possible boundary for the R_{snow} is to assume that the R_{snow} is always less than the time-averaged value of the spray flux, implying that the snow amount is never more than 50% of the total flux of water freezing. The brine salinity is then calculated by weighting the amount of fresh water from the R_{snow} and the saline sea-spray flux (R_w) relative to the total water flux. Moreover, there is a possibility that some of the snow will pass around the ship without hitting the vertical surface. However, for simplicity this effect is also neglected and a collection efficiency of unity is applied. The verification scores from a model including snow amount is also presented in the results section for the MINCOG adj model (MINCOG adj sn), since it has been left out of Paper III (Section 3.3).

On the contrary, contributions from other atmospheric sources have been fully neglected in the analysis. From Paper IV it is apparent that freezing rain does rarely occur in conjunction with icing in these sea areas. On the other hand, sea smoke or evaporation fog may be a contributing factor to icing, specifically in conjunction with sea spray. However, the water amount from such fog is challenging to estimate accurately, and is several orders of magnitude smaller ((0.01-0.2)$\times 10^{-3}$ kg m^{-3}) than those potentially obtained from sea spray (Table 2 in Makkonen (1984a)). However, when considering fog-droplet accumulation over several hours, the total water amount may be comparable to the time-averaged spray flux. In fact DeAngelis (1974) describes one event in the Barents Sea with

approximately 30 cm ice accumulation (12 inches) in 12 hours due to dense sea smoke.

2.3.9 Conductive heat flux (Q_{cond})

For steady growth of ice the conductive heat flux (Q_{cond}) through the ice layer and into the structure may be important in the beginning of the freezing process. The Q_{cond} may be expressed as follows (Kulyakhtin *et al.*, 2016):

$$Q_{\text{cond}} = k_i \frac{T_s - T_{\text{struct}}}{h} \tag{20}$$

k_i is the conductivity through saline-water ice which is in general lower than that of fresh-water ice (Rashid *et al.*, 2016). The temperature of the structure may for instance be set equal to the air temperature (T_a). However, since Q_{cond} is inversely proportional to the ice thickness (h), its effect will decrease with increasing ice thickness. In the 37 KVN events all ice thickness values are above 1 cm initially, and only 5 events are below 2 cm in the starting juncture of the accumulation period. According to Jessup (1985) the effect of Q_{cond} is negligible for ice thickness values below 1-1.5 cm.

If considering variable growth of ice during pulsed-spray condition, conduction provides an important contribution to the ice growth (Kulyakhtin *et al.*, 2016). The conductive heat flux will then come into play if assuming that there are periods between spraying in which the brine-surface temperature reaches equilibrium with the air temperature with a highly saline brine-water surface. In such situations there will be temperature gradients in the ice to which heat is conducted. A new portion of spray water with a much lower salinity than the brine-surface layer on top of the ice, will then contribute to ice accretion both due to heat released to the old accretion and to the net effect of the other heat fluxes considered on the right hand side of Eq. (5). Kulyakhtin *et al.* (2016) argue that this circumstance is observed in experiments conducted in Adventdalen in Svalbard at light cylinders in situations with spray periods exceeding 30 s. As argued in Paper II, considering the fact that a time-averaged continuous spray-flux is applied in the current study, and that the situation offshore on the vertical plate of KV Nordkapp might be quite different from the situation in Adventdalen in Svalbard in experiments at light cylinders, the effect of the conductive heat flux on ship-icing events are uncertain. Hence, steady ice growth is assumed, and the conductive heat flux is here fully neglected.

2.3.10 Summary of heat fluxes applied in MINCOG

When only considering the primary heat fluxes applied in MINCOG, the full heat equation (Eq. (5)) is reduced to:

$$Q_f = Q_c + Q_e + Q_d + Q_r \tag{21}$$

where

$$Q_f = L_{\text{fs}} R_i = L_{\text{fs}} \rho_i \frac{dh}{dt} \tag{22}$$

Spongy-ice accretion is included in the latent heat of freezing for saline water ($L_{\text{fs}} = 0.7L_f$) by considering the arguments from Makkonen (1987). A constant value of the ice density is also applied, although observed ice-accretion density is highly variable (Ryerson and Gow, 2000). Since spongy ice is considered, the density should probably incorporate brine which is stored in brine pockets before it migrates away from the accretion. In addition, a possible inclusion of snow may lower the density, and will further complicate the overall density calculation. The value of 890 kg m^{-3} derived from Stallabrass (1980) and applied in the current study is at least in the same ranges of the observed density values of Ryerson and Gow (2000) (693 kg m^{-3} to 917 kg m^{-3}).

The final icing rate (dh/dt) is calculated both at the start point and the end point of the junctures in consideration, and the average icing rate is calculated from the mean of the icing rate derived at the start and the end point when applying the KVN data. This calculated average icing rate is compared to the total ice accumulated during these junctures divided by the number of hours between them. An approach in which the mean values of the input parameters are applied in MINCOG and an icing rate calculated from these values are also tested (Paper II). However, the latter icing rates provide worse verification scores than the scores obtained when calculating the icing rate in the start and end point separately and then calculate the average icing rate from these two values. In addition, when applying the icing model in operational weather forecasting, the output parameters from numerical prediction models, which is applied as input to the icing model, are initially derived at each juncture and not as time-averaged values. Utilizing time-averaged variables from numerical prediction models may of course be feasible. However, it is more convenient to apply the parameters in the manner they are typically provided in. On the other hand, in the categorical verification procedure for the nomograms of Paper III the mean of the input parameters are applied as input to these statistical methods for icing-category determination, since the mean value of two severity categories, without any relationship to exact icing-rate values, are more difficult to interpret.

2.4 Verification of icing calculations

The advantage of the calculation of exact icing-rate values (continuous icing rate) is the fact that these are not contaminated by the thresholds selected or derived from particular ship types. Several verification scores are considered, and in Paper III the scores are compared to errors derived from a random-walk or naïv method in order to investigate whether the errors are lower than errors obtained from forecasts without skill.

The benefit of verifying the icing calculations in categories (categorical icing rate) is the possibility of allowing for some variation inside a certain category. This is particularly advantageous considering the notable uncertainties in both the modelled and observed icing rates. In addition, it is possible to include verification of no-icing events and compare the physical icing models with the icing nomograms in the categorical verification approach. However, the verification may be sensitive to the selected threshold values. For these reasons several variations of the thresholds are tested both in Paper II and Paper III. A multi-categorical approach is applied in the verification procedure by dividing the icing-rate observations in the four categories: no icing, light icing, moderate icing, and severe icing. Although most skill scores applied for categorical forecasts are developed for two categories only, e.g. equtiable threat score, there are also skill scores that are applicable for more than two categories. Since it is believed that a more complete verification is obtained by comparing several scores, the following four scores are all applied in Paper II and Paper III: Percent Correct (PC), Heidke Skill Score (HSS), Peirce Skill Score (PSS), and Gandin-Murphy Skill Score (GMSS). In Paper III these scores are also calculated when numbers are placed randomly in the selected categories with two sets of random distributions evaluated. In Paper IV only the two categories icing and no icing are tested, hence, equitable threat score and bias ratio are applied along with the scores used in the multi-categorical approach of the other papers.

Another interesting aspect to consider is the fact that there is no generalised standard of the thresholds for the categorical icing severity classes. Initially the same thresholds as applied in Overland *et al.* (1986) are applied in the current study (Paper II). However, it seemed also reasonable to generate new thresholds developed for the ships in consideration (Paper III). The idea is that the forecast for the KV Nordkapp ships may then be the reference for future icing forecasts issued in the marine-icing warnings. Furthermore, it is discovered that the frequency of occurrence for the icing rates above or below the selected thresholds developed for the KVN data, are quite similar for frequency of occurrence of the icing rates observed on the ships in the P&C and R&M data. However, the hazardousness experienced by a particular ship encountering a particular icing severity developed from frequency of occurrence may be different for a small ship compared to the large KV Nordkapp ship, i.e. moderate icing may be more dangerous for

smaller ships compared to larger ships although the frequency of occurrence is the same. Nevertheless, as emphasised in Paper III, there is at least some relationship between the hazardousness and frequency of occurrence for severe icing for the reference ship type in the method developed. The advantage of only considering icing and no icing events based on the weather situation as is done in Paper IV, is that the results probably are more ship independent and independent of the position on the ship in which icing has been recorded, than are the results considering icing rates.

3 Results

3.1 Paper I

Marine icing observed on KV Nordkapp during a cold-air outbreak with a developing polar low in the Barents Sea
Eirik Mikal Samuelsen, Sveinung Løset, Kåre Edvardsen, 2015. *Proceedings of the 23rd International Conference on Port and Ocean Engineering Under Arctic Conditions.* Norwegian University of Science and Technology, Trondheim, pp. 1-14.

Paper I is a case study of icing observations in conjunction with atmosphere and ocean parameters recorded on KV Nordkapp during a particular trip from Tromsø to Bjørnøya late February 1987. During the voyage KV Nordkapp accumulated 110 tons of ice based on readings from the ballast water. Icing recordings on the vertical plate between the fore deck and the cannon deck of the ship show a total accumulation of 20 cm in 17 hours. It is discovered that this particular event occurred during a weather situation where a synoptic low transformed into a polar low (Figure 6). This polar low appears to be a popular polar-low case with a hurricane-like form with an eye in the centre entitled in the literature as "a most beautiful polar low" (Nordeng and Rasmussen, 1992).

The icing event is analysed and calculations made for comparison between the observed and modelled icing rate on the vertical plate. Three different sets of icing models are evaluated: three variants of the Overland model (O1, O2, O3), there variants of the Modified Stallabrass model (M1, M2, M3), and three variants of a new proposed model named Test model (T1, T2, T3) which is a preliminary version of MINCOG. However, the test model assumes an elliptic shape of the perimeter of the ship when viewed from above, it neglects the radiative heat flux, it applies spray frequencies derived from fishing vessels, and it uses spray-cloud duration time from Lozowski *et al.* (2000). In addition, the droplet-cooling time is derived from a mean value between the version from Stallabrass (1980) and the spray-cloud duration time as applied in the Modified Stallabrass model. However, the Zakrzewski (1986)-formulation of spray-cloud duration time is applied in the Modified Stallabrass model. It is assumed that all droplets fly as individual droplets, and the spray temperature is set equal to the droplet temperature calculated from the droplet-cooling equation of Stallabrass (1980). For simplicity the heat-transfer coefficient applies the relative velocity normal to a cylinder instead of to a vertical plate, and uses only the transfer associated with the flow parallel to the plate (along-flow component).

The results show that for this particular event the Overland models and the Modified Stallabrass models overestimate the icing rates observed at this particular position on the ship. However, the variant of the Modified Stallabrass model

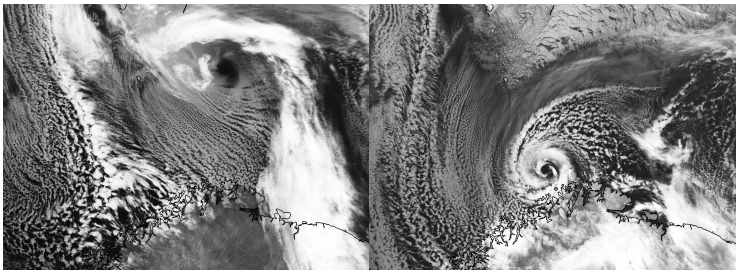

(a) (b)

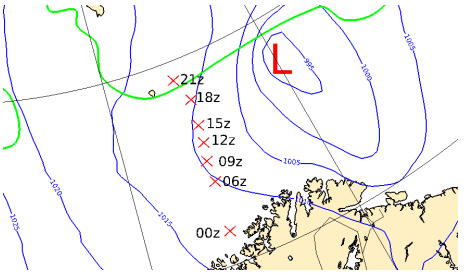

(c)

Figure 6: Satellite images from a) the synoptic low at 26 February 1987 1244 UTC, and b) the polar low at 27 February 1987 0418 UTC. The images are provided by NERC Satellite Receiving Station, Dundee University, Scotland (`http://www.sat.dundee.ac.uk/`). c) illustrates MSLP and ice-edge analyses made by the author with the bases of NORA10, of observed MSLP from the ship and synop stations in Northern Norway and in Svalbard, and of satellite-image information. The red crosses describe the position of the ship during 26 February 1987 in UTC or Z time.

(M3) that incorporates a time-averaging component in the spray-flux term, and a shorter droplet-cooling time than the other versions of the model (M1, M2), is more accurate. The different variants of the test model (T1, T2, T3) show similar performances as the M3 when compared against the observed icing rates from this particular event. Nevertheless, it is concluded that more evaluation is needed to state anything certain about the evaluation of the icing models.

Some results that were not presented in the paper, but is still relevant for the study as a whole, is a comparison between observed temperature and wind speed, and the temperature and wind speed derived from NORA10 and Arome Arctic 2.5 km. The NORA10 and Arome Arctic data are derived from the same position and juncture as the ship observations during the trip (Figure 7). The Arome Arctic 2.5 km model is run without data assimilation, but with ERA-Interim data (Dee *et al.*, 2011) at the boundary and at initial time. The applied model is a preliminary version of the currently-applied operational version at the Norwegian Meteorological Institute which is partly described in Süld *et al.* (2016). The main conclusion from Figure 7 is that both models are overpredicting temperatures and underestimating

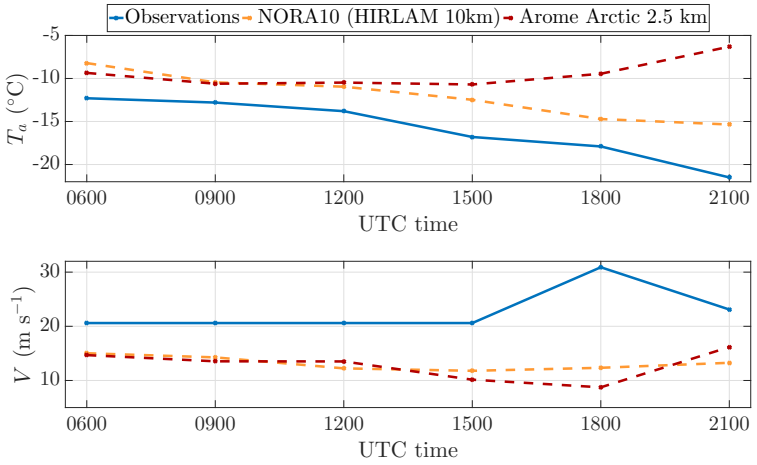

Figure 7: Comparison between observed temperature (upper panel) and wind speed (lower panel), and the 2 m temperaure and 10 m wind speed derived from NORA10 and Arome Arctic 2.5 km for the voyage in Paper I (Figure 6).

the wind speeds (BIAS of 3.8 °C in NORA10 and 6.4 °C in Arome Arctic for temperature, and BIAS of -9.6 m s^{-1} and -9.9 m s^{-1} for wind speed in NORA10 and Arome Arctic, respectively). Part of the overprediction in temperature of the Arome model may indeed be the fact that the applied version of the model is run without a sea-ice model, and only SST information from ERA-Interim is applied for sea-ice information. However, there might be other unresolved inaccuracies in the model as well. Part of the reason for the underestimation of the wind speed for both models is a misplacement of the centre of the low in the models. It is also apparent that the increased resolution apparent in the 2.5 km model compared to the 10 km model does not increase the forecast skill of the aforementioned parameters. However, a more detailed investigation shows that the high-resolution model has stronger winds than NORA10 near the centre of the low, but that the position of these strong winds are located east of the ship location (not shown).

An interesting aspect of Paper I is that this particular voyage encountered the most severe icing event documented in this sea area, at least among the ship-icing events investigated in this phd study. This particular severe-icing trip also arose in conjunction with one of the most severe polar-low events ever documented when comparing the violent-storm wind speed observed on KV Nordkapp with the wind speeds listed in a list of polar lows from Noer and Lien (2010) in the period between the years 2000 and 2010. When comparing this event to all polar-low events that arose from December 1999 to February 2017, this particular event will be ranked fourth of all the polar-low events ever documented (pers.comm., Gunnar Noer, Senior Meteorologist/Developer in Polar Meteorology at the Norwegian Meteorological Institute, June 2017). A possible relationship between severe icing

and polar lows has not been previously documented, and the possible relationships between snow fall arising along with such weather systems and icing are investigated in the extension of Paper III (Section 3.3) and in Paper IV.

3.2 Paper II

Modelled and observed sea-spray icing in Arctic-Norwegian waters
Eirik Mikal Samuelsen, Kåre Edvardsen, Rune Grand Graversen, 2017. *Cold Regions Science and Technology* 134: 54-81.

This paper focuses on all available data of icing rate from the three similar ships KV Nordkapp, KV Senja, and KV Andenes, which are entitled the KV Nordkapp class. In addition, 41 events with zero ice accumulation are added to the evaluation of the icing modelling. The test model of Paper I is further developed into a model named MINCOG. Two spray-flux expressions based on available spray data from the literature are applied in MINCOG. The formulation based on the Borisenkov spray data (Eq. (1)) is also applied in Paper I, but in Paper II the spray frequency is adjusted towards a large ship. The spray-cloud duration time from Paper I is also adjusted by finding a statistical relationship with a better fit than the verison of Lozowski *et al.* (2000) by investigating the spray-cloud duration-time data from Ryerson (1995). However, although the formulation is improved, the coefficient of determination is still not more than 0.22, which underlines the general uncertainty and randomness of the duration-time data. The other spray-flux expression, named the Horjen spray-flux formulation applied in Horjen (2013), is adjusted according to information from the Norwegian Meteorological Institute about wave heights and wave periods during the spray-collection expedition described in Horjen *et al.* (1986). Updated formulations utilising this new information provide better fit to the measured spray amounts than those applied by Horjen (2013). A mathematical expression for the gunwale of the ship is developed and applied for droplet-temperature and droplet-velocity calculations. The latter one is only applied along with the Borisenkov spray-flux expression. Radiative heat flux is included in the analysis, and for the first time short-wave radiative heat flux is incorporated in a marine-icing model. An updated expression for the heat-transfer coefficient towards a vertical plate is applied.

The main focus of the paper is to evaluate in which manner the application of a relationship between wind speed and wave parameters in marine-icing modelling affects icing calculation, and in which manner the use of NORA10 as input to the model affects icing-rate calculation in general. It is concluded that the application of wave height/wave period calculated from empirical relationships between wind speed and wave height/wave period, derived from data obtained from other regions than those in consideration, considerably worsen icing-rate predictions when these are applied as input parameters in MINCOG. This result is similar for both of the

two spray-flux formulations applied. Surprisingly the application of NORA10 as input to the model alone obtained satisfactory verification scores when compared to the scores obtained from using the main input parameters only from observations. However, the optimal input in MINCOG apparent from both continuous and categorical icing-rate verification scores is the use of observations in conjunction with NORA10 wave period and wave direction. It is believed that the observed wave period and wave direction are less accurate than those based on reanalysis data, since both of these parameters are visually estimated. On the contrary, the application of the visually-estimated wave height seems to be superior of the application of NORA10 wave height. A possible explanation for this apparent incoherence is the underestimation of the wind speed in some of the events in NORA10 (Figure 7), which will lead to an underestimation of the spray flux and the heat-transfer coefficient. A lower wind speed will reduce the spray flux both directly through the droplet speed, and indirectly through its effect on wave height. Finally, it is also concluded that the application of the Borisenkov spray-flux formulation in MINCOG provides more accurate results than the use of the Horjen spray-flux formulation for these events. This is mostly apparent for low waves, but there is also a question whether the extremely large spray-flux values apparent for the high-wave ranges are realistic. In fact, it is interesting to notice that the application of empirically-derived versions of the wave parameters from the wind speed is masking the inaccuracies apparent for the Horjen spray-flux formulation.

3.3 Paper III

Ship-icing prediction methods applied in operational weather forecasting
Eirik Mikal Samuelsen, 2017. (Under second review, by May 2017) *Quarterly Journal of the Royal Meteorological Society*

3.3.1 The results presented in the paper

Paper III builds on the results from Paper I and Paper II by fulfilling the evaluation of the methods practised in operational weather forecasting including MINCOG against the KVN data presented in Paper II. In addition, the models are evaluated against the P&C and R&M data from several ships in order to evaluate the applicability of these methods for several ship types. However, due to the uncertainty regarding the position on the ship in which the icing is recorded in these latter two data sets, the exact timing of the events, and the use of reanalysis data for some parameters with cruder spatial and temporal resolution than NORA10, the results of the evaluation of the models when applying these data sets should probably be given less weight than the evaluation from the KVN data. Continuous icing-rate verification and sensitivity tests are presented for six physical models, in which four of these are variants of the Overland model. Categorical icing-rate verifica-

tion is also applied in order to evaluate three icing nomograms that are widely used in operational weather forecasting. These nomograms are evaluated together with the six physical models in a multi-categorical verification approach. However, in contrast to Paper II which applies the boundaries from Overland *et al.* (1986) for icing-severity thresholds, new threshold definitions are developed between the three categories light, moderate, and severe icing based on frequency distribution of the icing-rate data. The new definition is mainly tuned against the KVN data, but the proposed frequency-based thresholds follow the frequency distribution of the icing-rate data from the other two data sets in a similar manner. However, the supplementary material includes evaluation of the methods against the old thresholds, and the original thresholds of the nomograms evaluated. Some verification scores from some additional variants of the Modified Stallabrass model and Overland are also included in the supplementary material.

The overall best verification scores for both continuous and categorical verification scores are obtained by MINCOG, and a physically-based Overland model updated from its initial version by applying a heat transfer based on the bulk-transfer method applied for heat-transfer calculations between the ocean and the atmosphere (see e.g. Fairall *et al.* (2003)). This Overland version also applies a higher freezing fraction in agreement with the calculations from MINCOG in Paper II, and includes formulations for both the evaporative and radiative heat flux. The radiative heat flux is calculated in the same manner as in the MINCOG model with longwave and shortwave radiation data derived from NORA10, but the surface temperature of the brine is set equal to the freezing temperature of the incoming sea water as in the other Overland models.

Sensitivity tests of the modelled and observed icing-rates for six important input variables, highlight that very low air and sea-surface temperatures rarely occur over sea areas together with high waves even for strong winds. This is further underlined by extracting temperature and wave data from 145,000 ship observations recorded in these sea areas. The observations show that wave heights above 4 m never occurred in this data set for temperatures below -20 °C. A possible explanation for this observed disjointedness between high waves and low temperatures is that such low temperatures only transpire near the ice edge, cold land areas, or even inside areas with fractional ice cover. Due to fetch limitations in these areas when the wind blows from the packed sea ice or land areas, high waves will not transpire even though the winds are strong. At least to the knowledge of the author this is a result that has never been highlighted in preceding marine-icing studies. For this reason it is preferable to apply ship-icing models or methods in operational weather forecasting that takes this effect into account by e.g. applying wind speed and wave height as separate input parameters.

3.3.2 The results of the MINCOG adj model not presented in the paper

As described in Section 2.3, the MINCOG adj model and two variants of this model: one with an added run-off parameter, and another one considering the effect of snow, are left out of Paper III. For this reason the verification scores for these models are included here. A model which applies the updated liquid water-content formulation of the spray flux in Eq. (4) is called MINCOG adj. A variant of this model which includes the run-off parameter in the Q_d term is named MINCOG adj ro, and another variant which includes snow fall derived from reanalysis precipitation data is named MINCOG adj sn. Total accumulated precipitation data are derived from NORA10 in the KVN data set, i.e. the total precipitation accumulation (R_R) divided by the number of hours of trip duration is applied for the start and end point individually in order to derive a precipitation-rate value (P_P). Daily-average precipitation-rate values (P_P) collected from North American Regional Reanalysis data (NARR) are applied in P&C and R&M. NARR data are provided by the NOAA/OAR/ESRL PSD, Boulder, Colorado, USA, and are collected from their Web site at `http://www.esrl.noaa.gov/psd/` (Mesinger *et al.*, 2006). It is assumed that all precipitation from the reanalysis data stems from snow.

The results of these three model variants including the result of the MINCOG model are summarised in Table 3 for the continuous verification scores and Table 4 for the categorical verification scores. When comparing the three adjusted model variants with the original version of MINCOG, it is apparent that the MINCOG adj has better verification scores than MINCOG for both continuous and categorical

Table 3: As Table IV in Paper III, but for the models MINCOG adj, MINCOG adj ro, and MINCOG adj sn not presented the paper. The original MINCOG model is also listed for comparison with the adjusted variants of the model.

Name	KVN data (N = 37)				P&C and R&M data (N = 47)				All three data sets (N = 84)			
	BIAS	MAE	RMSE	r	BIAS	MAE	RMSE	r	BIAS	MAE	RMSE	r
	†	††	††	†††	†	††	††	†††	†	††	††	†††
Ref.		**0.44**	**0.62**	**0.27**		**0.48**	**0.64**	**0.24**		**0.48**	**0.66**	**0.18**
MINCOG	**0.06**	0.50	0.64	**0.38**	**−0.12**	**0.36**	**0.52**	**0.42**	**−0.04**	**0.42**	**0.58**	**0.39**
MINCOG adj	**−0.05**	0.48	0.63	**0.42**	−0.18	**0.40**	**0.58**	**0.32**	−0.12	**0.43**	**0.60**	**0.37**
MINCOG adj ro	**0.06**	0.49	0.63	**0.54**	**−0.10**	**0.42**	**0.56**	**0.31**	**−0.03**	**0.45**	**0.60**	**0.43**
MINCOG adj sn	**0.08**	0.50	0.67	**0.44**	**−0.09**	**0.43**	**0.60**	**0.25**	**−0.02**	**0.46**	**0.63**	**0.34**

† Non-boldface is indicating that the mean error in the model is significantly (5% significance level) greater or lower than zero error (BIAS = 0). Boldface is indicating that there is not enough support from the data set to reject the null hypothesis that the BIAS in the model is greater or lower than zero (5% significance level) (see Paper III for details).

†† The 95 % lower limit of the ordered MAE and RMSE when applying a Monte-Carlo simulation ($N = 10^4$) of a naïv reference error (Hyndman and Koehler, 2006). Models with an MAE and an RMSE value below this reference value, have an MASE and an RMSSE significantly lower than 1 and these values are marked with boldface.

††† The 95 % upper limit of no positive correlation ($r = 0$) assuming t-distribution. Models with an r-value marked with boldface are greater than this highlighted reference value.

Table 4: As table V in Paper III, but for the models MINCOG adj, MINCOG adj ro, and MINCOG adj sn not presented the paper. The original MINCOG model is also listed for comparison with the adjusted variants of the model.

Modelname	KVN with no-icing (N = 67)				P&C and R&M (N = 47)				All data (N = 114)			
	PC	HSS	PSS	GMSS	PC	HSS	PSS	GMSS	PC	HSS	PSS	GMSS
New category definition												
Ref. (unif.)[†]	**0.34**	**0.11**	**0.13**	**0.19**	**0.36**	**0.12**	**0.16**	**0.33**	**0.32**	**0.09**	**0.09**	**0.14**
Ref. (obs.)[††]	0.42	0.13	0.13	0.14	0.53	0.18	0.18	0.14	0.37	0.10	0.10	0.10
MINCOG	**0.40**	**0.17**	**0.18**	**0.30**	**0.51**	**0.21**	**0.21**	**0.44**	**0.45**	**0.20**	**0.20**	**0.26**
MINCOG adj	**0.48**	**0.26**	**0.27**	**0.33**	**0.49**	**0.21**	**0.23**	**0.43**	**0.48**	**0.25**	**0.25**	**0.29**
MINCOG adj ro	**0.45**	**0.23**	**0.25**	**0.37**	**0.45**	**0.14**	0.15	**0.41**	**0.45**	**0.21**	**0.21**	**0.29**
MINCOG adj sn	**0.39**	**0.16**	**0.18**	**0.28**	**0.43**	0.10	0.11	**0.42**	**0.40**	**0.14**	**0.14**	**0.23**

[†] The 95 % upper limit of the ordered distribution organised from low to high of the different verification scores when applying Monte-Carlo simulations ($N = 10^4$) assuming that the predictions are uniformly distributed inside each category (see Paper III for details).
[††] The 95 % upper limit of the ordered distribution organised from low to high of the different verification scores when applying Monte-Carlo simulations ($N = 10^4$) assuming that the predictions are distributed in the same manner as the observations.

icing-rate verification for the KVN data set. For the other two data sets the continuous icing-rate scores are somewhat lower in MINCOG adj compared to MINCOG, while the categorical icing-rate scores are more similar. The overall effect when all data are merged together is better continuous icing-rate scores for the MINCOG, while the MINCOG adj has better scores for categorical icing rates. The effect of considering run off in the thermodynamics as described in Section 2.3.7 does not seem to enhance most of the verification scores for all data. This is apparent when comparing the results from MINCOG adj ro with MINCOG adj. However, the correlation coefficient is higher with than without run off, and the GMSS score is also higher in the MINCOG adj ro relative to MINCOG adj. In general the overall icing rate is increased in the MINCOG adj ro model compared to the MINCOG adj model, due to the reduced magnitude of the Q_d-term from the run-off effect. For this reason the negative BIAS in MINCOG adj for all data is reduced in MINCOG adj ro. Evidently adding snow amount from reanalysis data in the manner it is done here (MINCOG adj sn), is not increasing the accuracy of icing-rate predictions. This may imply that snow does not have a large effect on icing, but may also imply that the inaccuracies related to the collection of snow amounts as described in Section 2.3, hamper the possibility of evaluating the accuracy of including snow amounts in the model. Uncertainties related to accurate prediction of the spray-flux amount, may also reduce the accuracy of the icing-rate predictions when including snow in the model. An overall conclusion that my be drawn from the comparison presented here, is that MINCOG adj obtains the best verification scores for the most reliable data set (KVN). However, the overall quality differences between

particularly the upper three models of Table 3 and Table 4 are generally low.

3.4 Paper IV

Weather situation during observed ship-icing events off the coast of Northern Norway and the Svalbard archipelago
Eirik Mikal Samuelsen, Rune Grand Graversen, 2017. (Submitted, May 2017) *Tellus A: Dynamic meteorology and oceanography*

As emphasised in the results of Paper I, Paper II, and Paper III, there are uncertainties in the modelling of marine icing both within the models and in the parameters applied as input to the models. In spite of these inaccuracies it is probably still reasonable to apply modelling approaches like the one in MINCOG for short-term predictions of icing, specifically when applying wind speed and wave height as separate input parameters as is stressed in Paper III. However, forecast errors increase with increasing forecast lead time, and parameters near the lower levels in the atmosphere have higher forecast errors than those at higher levels. Thus, for predictions exceeding a couple of days it is preferable to apply fewer input parameters than those normally applied in marine-icing models, and input parameters obtained from levels less affected by the atmospheric boundary layer such as at 850 hPa. For these reasons Paper IV follows a more general approach by investigating the relationship between the weather situation and icing with emphasis on applying upper-air parameters for icing predictions. This is in fact one of the methods that was popular during the 1960s and 1970s among Japanese and Russian studies mentioned in Section 1.2.

In Paper IV icing and no-icing information from the R_S-parameter in the ship synop are utilised, and statistical relationships are developed between weather parameters and the icing/no-icing events from 17 ships operating in the Barents Sea, the Greenland Sea, and the Norwegian Sea in the period 1980 to 2006. When using the R_S-parameter for discrimination between the icing and no-icing events, no-icing events are arising in relatively similar weather situations as the icing events, since the icing protocol (Gr.22 in Figure 4) is only applied during icing-risk conditions. However, when $R_S = 1$ or 2 the observer has clearly noted some ice accumulating at that exact juncture, while when $R_S = 0$ such ice accumulation are not observed. In the middle of the summer season in which icing is not an issue, the observer does not register anything. On the other hand, there are also situations in the winter season where there is no information about icing in the synop log. For these reasons the R_S-parameter is found to be the best available discriminator between icing and no-icing events when not considering icing-rate severity as in the other papers.

A comparison between the data set in consideration and a previous study of Vasilyeva (1971) illustrates that in the present data there are more icing events en-

suing in cold-air outbreaks and in more severe weather conditions at the surface with stronger winds, lower temperatures, and higher waves. However, this circumstance may arise both due to the differences in the weather situation between these two periods in consideration (1965-1970 vs. 1980-2006), and due to differences among the ship types in the two data sets, i.e. the present study is investigating data for larger ships than the fishing vessels of the Vasilyeva (1971)-study.

Furthermore, map composites of mean values of the MSLP and temperature at 850 hPa (T_{850}) from all these events are generated. Vertical cross sections are derived by utilising the 40 model levels of the HIRLAM model used in NORA10. It is shown that cold-air outbreaks from the ice is the prevailing weather situation during icing. The mean of the MSLP field of both the icing and no-icing events illustrates a low pressure system situated in the Barents Sea with higher pressure in the Norwegian Sea and the Greenland Sea, and these weather systems are more intensified in the icing compared to the no-icing events. However, when investigating the weather situation in more detail it is revealed that around 10% of the icing events transpire in mountain-wave situations near the coast of Northern Norway and the Spitsbergen island in the Svalbard archipelago with a different flow pattern. Investigations of vertical cross sections illuminate how cold air upstream of the barrier is advected and partly accelerated downstream on the lee side of the large-scale mountains of Northern Norway and Spitsbergen island in the mountain-wave situations. Cross sections with humidity also indicate how the icing events in the easterly flow over Spitsbergen occur in more humid conditions than the conditions arising in the no-icing events which is an indication of more frontal activity in the icing events.

Moreover, the results of the paper in general support the investigations of Paper III that higher waves and stronger winds increase the risk of icing in sub-freezing conditions, and decreasing air temperature and decreasing sea-surface temperature do not increase the risk of icing alone in such conditions. Although the statistics are generated for all icing event independent of the cause of icing, the study highlights that sea-spray icing with or without snow is the most common cause of icing in these sea areas. An interesting finding is that freezing rain has rarely occurred as a cause of icing during the whole 27-year period on these ships. Furthermore, it is demonstrated that the risk of icing is higher when snow is observed, either as showers or frontal precipitation, which is underlined by cloud cover and relative humidity observations. However, it is not clear whether the precipitation in itself or the increased turbulence associated with showers and frontal wind intensification are the most important factors for the increased risk of icing in these events.

For a long-term prediction model for icing potential, a combination of a criterion for the temperature at 850 hPa (T_{850}) and a criterion for the temperature anomaly at the same level (ΔT_{850}) is suggested based on application of a logistic-regression method on a predefined training data set which contains approximately 2/3 of the whole data set. This model obtains better verification scores than ap-

plying criteria for 10 m wind speed and 2 m temperature, when all these variables are extracted from NORA10 and verified against a control data set of the remaining 1/3 of the data. A major drawback with this simple model is the problem of avoiding areas near the ice edge or inside fractional ice cover in which the waves are lower than further away from the ice edge due to fetch limitations. Hence the risk of spray-icing is lower in these areas than such a simple model indicates. On the other hand evaporation-fog or sea-smoke icing may still transpire in such areas even if the wave height is low. The wind speed will then probably determine whether the evaporation fog will arise above the free-board of the ship since the height of the evaporation fog according to Utaaker (1975) is dependent on the wind speed. Nevertheless, it is stated that more evaluation is needed with the use of long-term prediction prognoses with various variables to finally determine the optimal combination of variables applicable for long-term icing predictions.

3.5 Connection between the appended papers and the aims of the study (Section 1.3)

The different papers are developed in a sequential way. Paper I is an initial study with both data collection and verification for one particular voyage. The MINCOG model and the screened KVN data set of Paper II are developed by building on the results of Paper I. Paper II generates both a more accurate prediction method for ship-icing predictions in operational-weather forecasts, and generates a data set for model verification. Consequently, Paper III builds on both Paper I and Paper II by verifying all the models and methods applied in operational weather forecasting including MINCOG. The methods are verified against the data set of Paper II, and two additional data sets from several ship types. However, it is discovered that the icing-rate forecasts are still fairly inaccurate, particularly for usage in predictions exceeding a couple of days. Hence, Paper IV is developed from the basis of going back to the earlier and more general approaches of developing simple relationships between upper-air parameters and icing without considering the complexity associated with the physical modelling of the wave-ship-interaction icing process. Thus, the intention of Paper IV is to find simple associations between upper-air atmospheric parameters and icing to be utilised in long-term icing predictions.

As a consequence, R1 is effectuated through the case study of Paper I and the KVN data set of Paper II. R2 is achieved through the initial evaluation of Paper I which is fulfilled in Paper III. The evaluation of input parameters in R3 is mainly realised in Paper II. R4 is accomplished through the sensitivity tests of important input parameters to icing rate in Paper III, and in a more general approach evaluating the weather conditions in icing and no-icing events in Paper IV. A short-term icing-prediction method of R5 is suggested in Paper II with the application of new thresholds between the icing-severity categories in Paper III. Paper IV proposes a method for application in long-term prediction of icing (R5).

4 Discussion

4.1 General discussion

The main focus of this phd thesis as a whole is to investigate icing from an operational-weather-forecasting perspective. Firstly, evaluate the quality of current methods practised by operational weather forecasters by collecting testable icing data in conjunction with atmosphere and ocean parameters, and secondly, develop better forecasting methods if possible. In addition, investigate in general the relationship between weather parameters and icing including the weather situations in which the icing events ensue in the Arctic-Norwegian waters. It is interesting to notice that the initial case study of Paper I, partly delves into many of these aspects. Paper I sets the standard for utilising icing, atmosphere, and ocean data from the KV Nordkapp ship, which results in the unique KVN data set presented in Paper II. Furthermore, Paper I indicates that the Overland model and the ModStall model applied in operational weather forecasting are overpredicting icing, which is supported by the more comprehensive verification study of Paper III. Next, Paper I shows a possible relationship between polar lows and icing, which is supported by Paper IV where it is highlighted that icing occurs most frequently during cold-air outbreaks in these sea areas. The extension of Paper I illustrated in Section 3.1 of the thesis, also highlights the potential problem of applying reanalysis data or other high-resolution atmospheric model data for icing prediction for one particular situation. However, Paper II states that this is not a general problem when comparing the verification scores of all the KVN events applying NORA10 data as input to MINCOG with other variants of model input.

4.2 Application of the phd study

4.2.1 Short-term icing prediction

One of the outcomes of the study is the model of MINCOG for application in short-term predictions of icing. A preliminary version of MINCOG is described in Paper I (T1), and this version is currently implemented in the forecasting tool of MET Norway. As input parameters a model system is applied which is a combination of numerical prediction models for the atmosphere, the ocean waves, and other ocean variables. These three model types are at the current stage not coupled, but the goal is that the icing model at a future stage uses input parameters from a fully-coupled model system. In the Arctic region the following system of models is currently applied: a high resolution atmospheric model named Arome Arctic 2.5 km (Süld *et al.*, 2016), a wave model named MyWave with 4 km horizontal resolution which is a further development of the WAM model described in

Günther *et al.* (1992)[5], and an ocean model called Nordic 4 km which is partly described in Lien *et al.* (2013)[6]. From the atmospheric part of the model system the $V_{10\mathrm{m}}$, $T_{2\mathrm{m}}$, MSLP, and the R_H or dew point temperature at 2 m are applied as input to the icing model. From the wave-modelling part the H_s and P_s are used. From the ocean model the SST, sea-water salinity (S_w), bathymetry data, and sea-ice information are all applied. It is determined to set those areas in which the sea-ice concentration is greater or equal to 0.4 to not have a defined icing-rate value, and those areas in which some of the input parameters are not defined will nor have a value for the icing rate. The ship parameters vessel speed (V_s), the angle between the wind and ship direction (β), and the angle between the wave and ship direction (α) are all set to constants equal to the mean or the median value of the values observed in the KVN data set described in Table 2 in Paper II (V_s = 4 m s^{-1}, $\beta = \alpha = 150\,^{\circ}$). A different option is to calculate the β and α by utilising the wind and wave direction derived from the numerical prediction models for various pre-defined ship directions. An example of a particular prediction using the aforementioned model system as input to the Overland model and the T1 version of the MINCOG model (Paper I) is illustrated in Figure 8. This figure shows a short-term 12 h prognosis from 6 March 2017 for an area northwest of Svalbard. Since the Overland model is more sensitive to SST than other parameters (Paper III), particularly wave height which is not applied as input to the model, it is apparent that this model provides higher icing-rate predictions in the areas near the ice edge. It is also noticeable that the left part of the lower-panel figure with the Overland model displays an area with no icing in which the T1 model (upper panel) has light icing. This circumstance occurs due to the high sensitivity of the Overland model to SST since the highlighted area in this particular situation has an ocean stream of relatively high sea-surface temperature towards the northwest in the Nordic 4 km ocean model. From the results of Paper I and Paper III it is believed that the T1-model prognosis or the later MINCOG-model prognosis do provide a more realistic description of the icing conditions than do an Overland prognosis in such situations. However, the accuracy of the icing prediction is also dependent on the quality of the model-input parameters which is not evaluated in the current study. It should also be notable that the icing-severity thresholds are based on the frequency distribution of icing-rate observations of the KV Nordkapp ship type, implying that

[5]The operational high-resolution ECMWF model is used as the atmospheric-forcing model in the Arctic region (ECMWF, 2015).

[6]For the areas south of Bjørnøya a different model system is applied: the AROME MetCoOp for the atmosphere (Müller *et al.*, 2017), and MyWave for the ocean waves with 4 km horizontal resolution. In some areas near the coast MyWave with 800 m horizontal resolution is applied. Winds are derived from the AROME MetCoOp model in all these wave models. Finally, a high-resolution ocean model named NorKyst800-ROMS with 800 m horizonal resolution is used near the coast of Norway, and the Nordic 4 km model is applied elsewhere. Both of these two ocean models are connected to the Regional Oceanic Modeling System (ROMS) (Shchepetkin and McWilliams, 2005).

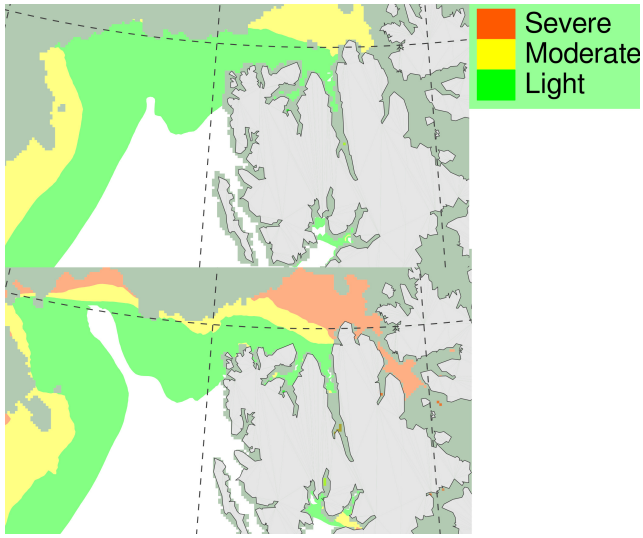

Figure 8: 12 hour prognosis of icing from 06 March 2017 when applying a preliminary version of the MINCOG model named T1 in Paper I (upper panel), and the Overland model from Overland (1990) (lower panel). The thresholds between the icing severity categories proposed in Paper III is applied for both models. The model system applied as input to the icing models is the Arome Arctic 2.5 km model, a wave model with 4 km horizontal resolution named MyWave, and the ocean model Nordic 4 km (see text for details). A constant vessel speed of 4 m/s and an angle between the ship and wind of 150 °, which are the mean values of the KVN data in Paper II, are applied. Grey shadings illustrate areas in which icing rate is not calculated due to high sea-ice concentration or non-defined input parameters of the icing models.

severe icing in general should only be observed in around 10% of the icing events, moderate icing in around 40% of the icing events, and light icing in 50% of the icing events related to a particular position on these large ships. This implies that the position in the front of the KV Nordkapp ship is currently seen as a reference position on a reference ship for the severity thresholds forecasted. On the other hand, as mentioned in Paper II, the position is only maximum 20 m from the bow and not in the back of this 105 m long ship, and the bow shape when inspected from the side has a similar shape as the medium-sized russian fishing vessels illustrated in Zakrzewski and Lozowski (1989), and the Endre Dyrøy ship illustrated in Horjen *et al.* (1986). For these reasons the reference-icing observations to which the thresholds are tuned, may be applicable for other ships as well. Furthermore, if regularly icing-rate observations is developed for smaller ships with lower freeboards, particularly fishing vessels, it may be possible to test whether the icing-rate observations on this large ship are applicable for the smaller ships. If it is revealed that the KVN-calibrated thresholds are not suitable for such ships, it is also possible to develop thresholds more appropriate for smaller ships by applying the same techniques as in Paper III. Nevertheless, it is at least manifested in Paper III that

similar icing-rate frequencies are experienced for the group of ships with various sizes from the P&C and R&M data sets. Another aspect to consider is that even though the forecast is developed for a particular juncture, the verification is based on ice accumulation up to nine hours for the KVN data, and 12 hours for the P&C data. For the R&M data the duration of the event is unknown. This implies that in order for a particular ship to experience the predicted icing rate, it is assumed that the conditions are constant some hours ahead in time. A possible solution to this inconsistency may be to collect output values from the numerical-prediction models with a relatively high frequency for a certain set of hours ahead in time, e.g. three-hour intervals. Furthermore, average values of the parameters obtained from these hours may be calculated and applied as input to the icing model instead of only applying the values from the particular junctures. An additional possibility may then be to consider time variation in the meteorological variables during these hours, but then the time variation in the ship movement, spray generation, and the freezing process should also be considered. As previously emphasised, this will dramatically increase the complexity of the model, and more icing and spray observations need to be collected in order to verify whether such complexity enhances prediction accuracy.

4.2.2 Long-term icing prediction

The high-resolution numerical-prediction models do not provide data for more than a couple of days ahead. For predictions with longer time spans output from the ECMWF model from the atmosphere and the ocean waves may be applied, and the slower changing variables as sea-water salinity, bathymetry, and sea-ice concentration may be set to fixed values (both temporally and spatially constant) if the forecast period exceeds the ocean-model forecast range. In addition, for more accurate long-term predictions it is preferable to apply ensemble-prediction models rather than deterministic models. However, as highlighted in Paper IV, instead of doing intricate icing calculations in models with many input parameters and partly inaccurate physical descriptions, it might be preferable for long-term predictions to simply apply criteria of the temperature and temperature anomaly at 850 hPa to provide an indication whether there is a risk of icing or not. Paper IV describes how the application of these upper-air parameters are more advantageous than just applying the freezing temperature of the incoming sea water obtained from $T_{2\mathrm{m}}$ and a threshold of around 10 m s^{-1} wind speed from $V_{10\mathrm{m}}$ when these are derived from NORA10. An example of predictions with T_{850} and ΔT_{850} from 22 February 2017 valid for the sea areas near the city of Tromsø is illustrated in Figure 9. If applying a criteria for icing when $T_{850} \leq -15$ °C and $\Delta T_{850} \leq -4$ °C suggested by Paper IV, it is apparent that there is some risk of icing in the beginning of the prediction period of this figure, but probably no risk or very little risk of icing for the next 14 days. The climatology period of the T_{850} applied in Figure 9 is the last 30

years from the GFS model rather than the 27-year period of 1980 to 2006 provided by the NORA10 data in Paper IV. Thus, the exact numbers indicating icing risk might be different when applying the GFS model than the criteria developed from NORA10 data. Nevertheless, the figure exemplifies how such predictions from the parameters T_{850} and ΔT_{850} may be applied. The information about the possibility of precipitation in the beginning of the prognosis along with a $T_{850} \leq -15$ °C and $\Delta T_{850} \leq -4$ °C, enhances according to Paper IV the risk of icing. However, the accuracy of the precipitation prediction dramatically decreases with increasing forecast lead time, and the precipitation information is probably not accurate enough to be applicable in the end of the described forecasting period in Figure 9.

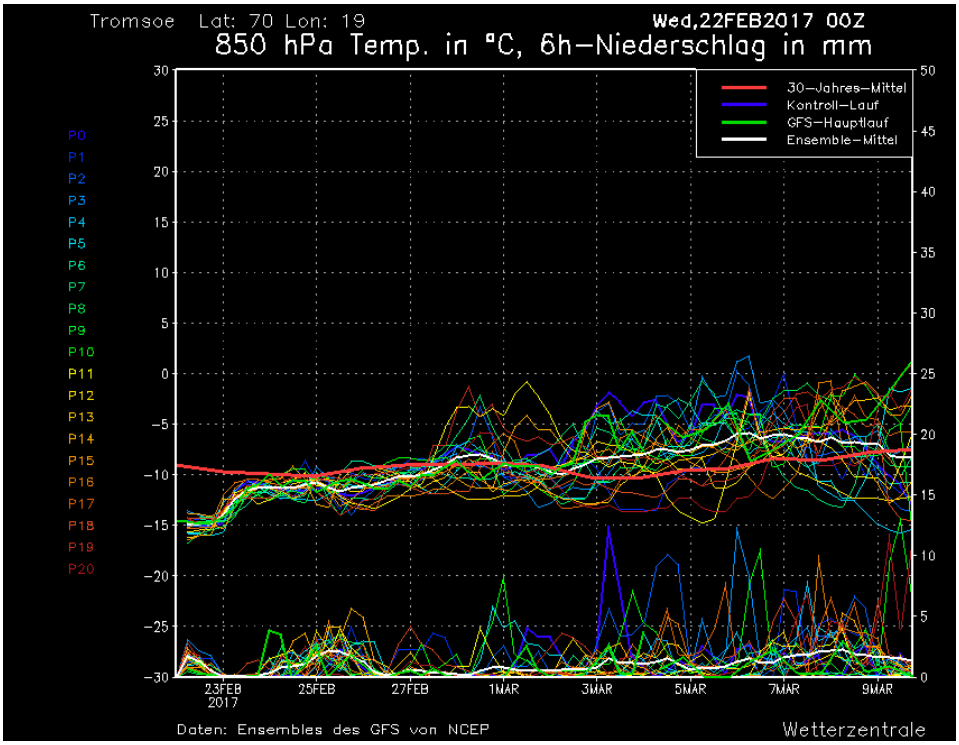

Figure 9: Example of a 15-day prognosis of temperature at 850 hPa level above Tromsø in Northern Norway issued at 22 February 2017 provided by the ensemble prediction system of the GFS model (NCEP, 2017) (Source: `www.wetterzentrale.de`). The red line visualises the mean value of the model climatology from the last 30 years, the green line shows the operational GFS model, the blue line describes the control run with same resolution as the 20 other perturbed runs shown with different colours, and the white line shows the mean value of all the 21 runs. T_{850} values are described on the left y-axis in °C. At the bottom of the figure, six-hour-accumulated-precipitation ensemble forecasts are provided, and the values in mm are described on the right y-axis.

4.3 Icing ensemble prediction system

For the short-term prediction of icing with MINCOG there is also a possibility to utilise input parameters from short-term ensemble prediction models as suggested in Paper III. It might then also be advisable to apply ensembles or different variants of uncertain expressions or variables in the icing model as well. In the following section some suggestions are provided how the variables or expressions applied in MINCOG may be perturbed.

4.3.1 Spray temperature

The spray temperature may be set equal to values in the ranges from the SST to the droplet temperature calculated from the droplet-cooling equation described in Paper II. The droplet temperature of individual droplets may be calculated by applying a minimum droplet cooling time equal to a minimum value of s/W_r (assuming a straight trajectory in the reference system of the boat), and a maximum value equal to the expression for the spray-cloud duration time provided in Paper II. It might also be possible in the calculation of the droplet temperature to apply the probability density function (PDF) of the observed droplet sizes from the observations described in Ryerson (1995).

4.3.2 Spray flux

There are many possibilities for variations in the spray-flux term. For the liquid water content of the spray-flux formulation derived from the spray data of Borisenkov *et al.* (1975), some variants derived from Zakrzewski (1987) and Roebber and Mitten (1987) have already been presented in Paper I, Paper II, and in Eq. (4). The formulation of the spray-water content applied in Kachurin *et al.* (1974) may also be applied if assuming that the spray data utilised for the development of this water-content expression ($l_{\mathrm{wc}} = 10^{-3} H_s$) were collected at the deck level, and with a similar exponential decrease with height as in the other formulations. For spray frequencies it is possible to apply both the empirical formula from Panov (1971) applied in Paper I for fishing vessels, and the formula for a larger vessel applied in MINCOG (Paper II). For spray-cloud duration time it is possible to apply the proposed formulation of MINCOG derived from the observed spray-cloud duration time data of Ryerson (1995), or simply use the observed ranges from the same data set of Ryerson (1995) (0.5 s to 6 s). Due to the uncertainty of the time-duration data it may in fact be set to fixed values independent of the environmental conditions. As spray speed the horizontal wind speed relative to the vertical plate may be used, or various calculations of droplet speed from the mathematical formulation of Paper II for different droplet sizes. However, according to Finstad (1995), for droplets below a value of around 0.5 mm, there is a greater chance for the droplet to be deflected around the ship instead of hitting it. In order

to consider this effect a collection efficiency may be added to the R_w-expression based on the droplet size for flows around flat plates. Such an expression is erroneously applied in Paper I for the large droplets with sizes of 2 mm. However, for such large droplets gravity will be more important than the effect of deflection. Finally, it is possible to both apply a model with and without the run-off term, and even vary the run-off term (a_{ro}) from values within the range 0.25 to 1, hence adjusting the effect of the Q_d-term as described in Section 2.3.7. Finally, it is also possible to add the effect of snow in some of the perturbations as exemplified in Section 2.3.8.

4.3.3 Heat-transfer coefficient

Several formulas for the heat-transfer coefficient has been evaluated in this study (Paper I, Paper II, Paper III). All these variants including the Bulk formula suggested in a variant of the Overland model in Paper III may be applied in an ensemble prediction system. In addition, the proposed formulation of Kulyakhtin and Tsarau (2014) for the heat-transfer coefficient for a 90 m wide offshore rig column derived from CFD modelling may be applied if using $D = 4$ m, and the formulation proposed by Hansen and Teigen (2015) for flows towards vertical plates based on the formula of Defraeye *et al.* (2010) may also be used. Sensitivity tests of all these variants of the heat-transfer coefficient to wind speed are provided in Figure 10 when applying the mean values of the parameters from the observations in Table 2 in Paper II for the other parameters. For the Bulk-transfer coefficient the following expressions are plotted in Figure 10: one assuming neutral conditions as applied in Paper III, and another version using the calculated Bulk-Richardson number (e.g. Eq. (5.6.3) in Stull (1988)) applying the mean values of SST and T_a from the KVN data. As illustrated in Figure 10, there are not large differences between these two formulations, implying that the assumption of neutral conditions does not yield a large effect on the calculated heat transfer compared to considering the unstable static stability generated by the large temperature difference between the ocean surface and the atmosphere. The in general main message with this sensitivity plot is to illustrate the differences between various formulations for the heat-transfer coefficient (Figure 10). For different angles between the wind and ship, there will be variations in specifically the curves of the formulation of Kulyakhtin and Tsarau (2014), Hansen and Teigen (2015), and Paper II. From Fig.13 in Paper III it is suggested that there should be some sensitivity to this angle according to the observations, but more observations are needed to clarify the exact sensitivity. The otherwise most striking signature of the figure is the different shape of the curves of the Bulk-formulation assuming a Reynolds-number independent flow, and the other formulas assuming a heat-transfer coefficient approximately proportional to

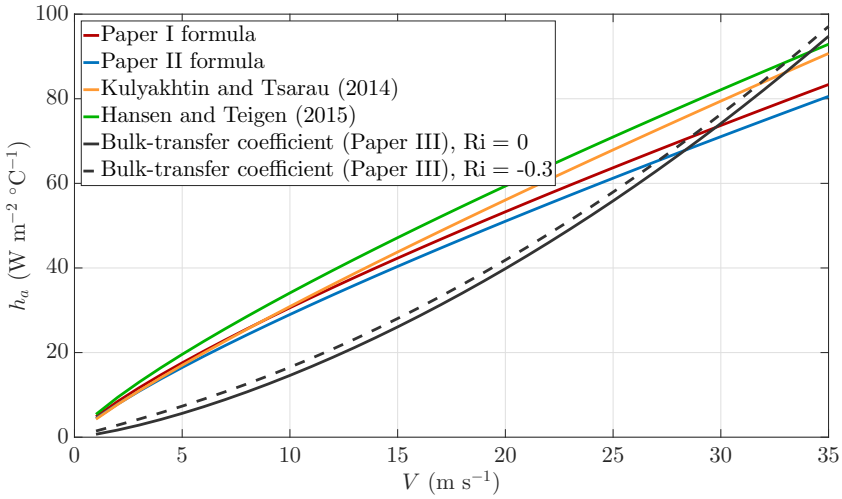

Figure 10: Sensitivity test of different formulations of the heat-transfer coefficient to wind speed for otherwise constant conditions using the average of the observed values in Table 2 in Paper II.

$\mathrm{Re}^{0.80}$-$\mathrm{Re}^{0.86}$ for a turbulent flow [7]. Moreover, the application of the Bulk formula does not consider the vessel speed, but assumes that the eddies that govern the heat exchange between the ocean and the atmosphere, also will affect the heat exchange between brine surfaces on a ship and the atmosphere when the ship is travelling through an area with such eddies. The other heat-transfer-coefficient formulations are suitable for calculations on more specified components of a ship on a smaller scale, but only when assuming forced convection alone. A draw-back with the latter formulations is that for instance variations in the surface roughness due to changes in the surface roughness of the ocean waves are not considered as is done in the Bulk formulation (Paper III). As a matter of fact the formulation of Defraeye *et al.* (2010) is simulated over a grassland with an assumed surface roughness (z_0) of 0.03 which is quite far from the smooth ocean surface with $z_0 \sim 10^{-4}$ to 10^{-3} (Table 3.1 Foken and Nappo (2008)). However, the roughness of the components of the ship may increase the surface roughness for the ship-icing problem to be closer to the grassland roughness.

4.3.4 Radiation

Different weighting of the various components important to the incoming long-wave radiation may be applied in order to perturb the calculations (Eq. (15)). The

[7] The Re-numbers considered in the study are of the order 10^6 which is greater than a criteria of 10^5 suggested by Lienhard IV and Lienhard V (2008) for the onset of turbulence in a controlled environment. In addition, the static instability encountered during icing conditions would lead to negative Richardson numbers and anyhow generate turbulent eddies affecting the flow.

short-term radiation may be added for various view factors by changing the tilting angles, i.e. from a vertical to a horizontal view.

4.3.5 Summary

Adding all this information together will then provide a super ensemble with possible probability information for a forecast of a particular icing-severity category. However, it is a chance that the spread of such a super ensemble will be too large to provide the needed sharpness of such forecasts. Adding more weight to the variant of the physical parameterizations applied in MINCOG compared to the other perturbations, may be a solution for some of the terms added and may increase the sharpness of the forecast. At least when such a model, which includes all these model variants suggested, calculate a 100% probability of the extreme cases: no icing or severe icing, it is a more accurate forecast, than a prediction of these events from a deterministic icing model alone. Maybe a combination of such an ensemble model system and a deterministic model will provide the most suitable information for the end users.

4.4 Possible improvements

4.4.1 Wave-ship interaction derived from wave-spectrum data

Although there are many aspects considered in the current study, there are also many aspects that are left out which might need more consideration. First and foremost, better understanding is needed regarding the interaction between ship and waves. In the present study simple relationships are applied which links the significant wave height, wave period, mean wave direction, and bathymetry data, with the spray amounts encountered on a ship with a certain mean velocity during two junctures. Instead of applying such wave parameters developed for visual wave-height or wave-period estimation, utilising wave-spectrum data from high-resolution wave models may be an alternative. If measurements of wave spectra using e.g. radar technology are feasible, such data may be combined with spray measurements. It will then be possible to investigate if more accurate spray-flux formulations are obtained between the wave parameters and the spray data. However, it is important that such measurements are recorded in a variety of conditions including extremely high waves in order to establish more generalised empirical relationships. Paper II highlights for instance how the spray-flux formulations of Horjen (1990) and Horjen (2013) probably are not applicable outside the wave-height ranges encountered during the spray-collection cruise described in Horjen *et al.* (1986).

4.4.2 Considering ship dynamics

A major simplification in the MINCOG model is the negligence of the movement of the ship in the six degrees of freedom on top of a pure horizontal translation. Heave, sway, surge, pitch, roll, and yaw may considerably affect both the spray collected, the droplet trajectory, and hence the droplet-cooling time, spray frequency, and even mechanical break-off of the ice. Whether it is realistic to assume that such effects may be incorporated in an icing model for application in operational weather forecasting, is a different question.

4.4.3 The effect of wind-driven spray

The contribution of droplets detached from the top of the wave crest during strong wind conditions, entitled wind-driven spray, is not considered in this study. The application of formulas for wind-driven spray provided by Wu *et al.* (1984) used in e.g. Horjen (1990, 2013, 2015) yields spray fluxes up to not more than 0.6 g m^{-2} s^{-1} even for 30 m s^{-1} winds (Fig.4 Horjen (2015)). This is approximately one order of magnitude lower than the median values of the time-averaged wave-interaction spray fluxes calculated in the MINCOG model for various sets of input parameters presented in Table 3 in Paper II for the Borisenkov spray-flux expression. However, the exact spray-flux amounts from wave-ship interaction icing may be highly variable as suggested by the spray-flux derived values of the spray data from Horjen *et al.* (1986) presented in Table B.1 in the Appendix B of Paper II (0.1 to 10.9 g m^{-2} s^{-1}). The calculated wind-driven spray values mentioned here are also uncertain, and the applicability of the formulation from Wu *et al.* (1984) above 7 m above the sea level is questionable according to Horjen (2015). Jones and Andreas (2012) suggest that large spume droplets may contribute considerably to freezing at an offshore rig for winds above 19 m s^{-1}, assuming that all droplets freeze on impact. However, Kulyakhtin and Tsarau (2014) argue that the contribution in general from wind-driven spray is low since the droplets have high salinity values since they are evaporating during their flight. Thus, the freezing temperature of the droplets will be lower than a value of around -20 °C according to Kulyakhtin and Tsarau (2014). This implies that the wind-spray droplets are mostly not supercooled since they then in most instances have a temperature above their freezing temperature. In addition, Kulyakhtin and Tsarau (2014) argue that droplets in wind-driven spray will have low inertia and therefore most of the droplets will be deflected around and not hitting the structure. On the other hand, strong conclusions regarding such effects may not be drawn, since the actual turbulent wind field during the statically unstable conditions in icing events are probably different from the turbulent wind field modelled by the CFD models of Kulyakhtin (2014). These CFD models are namely not considering convection or showers. The evaporation effect and salinity content of the droplets must also be further in-

vestigated in order to conclude whether the claim of Kulyakhtin and Tsarau (2014) is correct. Therefore more observations of wind-driven droplets must be collected in order to evaluate the properties of wind-driven spray and conclude whether the negligence of this spray component is feasible or not. For the empirically-derived spray-flux formulations applied in the current study, it is believed that possible wind-driven spray is partly included in such formulations due to the fact that all types of spray collected during the excursions are probably incorporated in such spray data. However, since neither the spray data of Horjen *et al.* (1986) nor that of the Borisenkov *et al.* (1975) were recorded in conditions for winds above 19 m s^{-1}, there might be a higher contribution from this type of spray for stronger winds than the applied formulations take into account. This may in particular be a fact if rising motion and turbulence in conjunction with showers or mountain waves, e.g. in hydraulic-jump features downstream of the sometimes observed downslope windstorms during offshore flows at the coast of Northern Norway (Samuelsen, 2007), may lift larger droplets to even higher elevations than what is suggested by the spray-concentration formula of Jones and Andreas (2012).

4.4.4 Data collection

Spray and icing data for various parts of the same ship should be measured with higher precision. Both the spray and icing amount may vary considerably both horizontally and vertically for the ship in consideration. In order to be able to develop better models for both the spraying and the icing of a ship, all these parameters should be measured at various locations on the ship in conjunction with weather and ocean parameters in order to investigate the horizontal and vertical differences in these variables for a vast range of weather conditions. If this is achieved it will be possible to establish more accurate empirical relationships between the weather parameters and the spray amounts collected and frozen. The salinity of the spray should also be measured in order to derive the amount of fresh water mixed into the spray either from evaporation fog or snow. Turbulent measurements with for instance high-frequency three-dimensional sonic anemometers in order to extract eddy-flux covariances at various location on a ship, may be used for more accurate heat-transfer estimations.

4.4.5 Combining numerical prediction models for the atmosphere and ocean with CFD models

Finally, an additional idea is to utilise the temporal and spatial variation in the numerical-prediction models of the meteorological society as input to the CFD models of the engineering society to calculate icing on ships or structures at specific locations. This may be done if it is possible to update the boundaries of the CFD with data from the numerical prediction models of the atmosphere, ocean-

wave, and the ocean from the new position of the ship at a future time step. However, more interdisciplinary research between meteorologist and engineers are needed in order to run such model systems. Vast amount of resources and close collaborations between researchers associated to both environments are probably needed for such projects to succeed in order to secure better data collection and more accurate modelling approaches.

5 Conclusions

Ship-icing issues have been investigated for more than 60 years, and will probably be further investigated for many years in the future as long as shipping sustain in cold marine climates. Although better and less cost demanding de-icing techniques may reduce the risk of icing at sea, total sheltering of sea-spray in conditions with extreme winds, waves, and low temperatures is difficult to achieve. A recent experience by the Norwegian Coast Guard encountering storm conditions and high waves in temperatures as low as -19 °C in the Barents Sea, is that spray icing is still encountered on their modern ice breaker KV Svalbard with mounted heating cables in such weather conditions (yr.no, 2017a). In the weather windows and after the icing episode the soldiers had to hammer the ice lose with mallets as the one in Figure 1 in the old-fashioned way and throw the ice lumps off the ship (Front-page illustration).

A major conclusion from the study as a whole is that it is possible with simple adjustments to the methods applied in operational weather forecasting to generate a model with higher accuracy. More detailed findings, contributions, and conclusions extracted from the study may be listed up as follows:

- A unique data set is generated with both icing data and necessary input parameters for application in model verification. This is probably the most comprehensive data set ever applied in icing modelling.
- A completely new model for application in operational weather forecasting is developed. This model is entitled MINCOG and is adjusted and evaluated against icing-rate observations on a particular position on the KV Nordkapp ships.
- Unprecedented thresholds for the icing-severity categories based on frequency of the icing-rate data are derived. Interestingly the old nomogram of Mertins (1968) achieves higher verification scores when these new thresholds are applied compared to the scores obtained from using its original thresholds.
- Wave parameters like significant wave height and wave period derived from empirically-based relationships between wind speed and these parameters should be avoided in icing-modelling approaches.
- The Overland (1990) model which is widely applied in operational weather forecasting, greatly exaggerate icing-rate predictions and should be replaced by other methods. The reason for this overprediction is in fact that the application of this model, although the model is claimed to be empirical, is similar to applying a model with an unrealistic large heat-transfer coefficient. This effect is in most regions partly masked by a very large heat flux from the sea

water, due to an assumption that only a small fraction of the incoming sea water freezes. However, for low sea-surface temperatures extreme values for icing rates are encountered. Although it is stated by Overland (1991) that the model may not be applied in areas which are not open ocean, and applied only for forecasting icing in categories, the model challenges is still apparent specifically when numerical prediction models are applied as input to the model. It is also found that there might be an underestimation of icing in areas with relatively high sea-surface temperature due to the heat in such conditions from the vast amount of water estimated by the model (Figure 8).

- Notable improvement of the Overland model is apparent when using a physical model with a heat-transfer coefficient calculated from a bulk-transfer coefficient for the heat exchange between the ocean and the atmosphere, adding the effect of evaporative and radiative heat fluxes to the model, and using a higher freezing-fraction value based on model calculations from the MINCOG model.

- Wind speed, wave height, and the angle between the wind and ship directions are the most important parameters for icing predictions in sub-freezing conditions. Observations of icing show that low air-temperatures are mostly an important factor in relationship with these parameters, and not alone, when considering already sub-freezing conditions.

- High waves ($H_s > 4$ m) and very low air temperatures ($T_a < -20\ ^\circ$C) are rarely observed in conjunction, implying that nature sets a limit to the degree of wave-ship interaction icing that may arise at sea. For this reason models that are not using wave height as a separate input parameter will exaggerate icing-rate predictions in fetch-limited regions for strong winds. This is a highly unprecedented result, and explains why there is a drop in both the severity of icing for low air temperatures (Lundqvist and Udin, 1977), and why the frequency of icing compared to no-icing is lower at such temperatures. This contradicts some claims in the early literature presented in Shellard (1974) that sea-spray droplet freezes in the air before hitting the superstructure of a ship at a temperature below $-18\ ^\circ$C as an explanation for the observed drop in severity and frequency of icing at low air temperatures.

- Sea-spray icing is the major cause of icing in Arctic-Norwegian waters, but the presence of snow showers or frontal snow increases the risk of icing. However, it is uncertain whether the increased turbulence associated with the presences of fronts or showers, or the snow amount and the cooling effect from the snow fall by itself, are the most important factors for this increased risk apparent in this study. One of the reasons for this uncertainty is that accurate model calculations of the effect of snow fall on icing and

accurate and quantifiable snow amounts derived from observations at sea during icing events are both difficult to obtain.

- Sea-surface temperature has limited effect on icing as long as the sea-surface temperature is in the ranges observed in Arctic-Norwegian waters. In fact it is observed that icing arises in areas with a slightly higher sea-surface temperature than areas without a registered ice accretion derived from the synop code. Although a lower sea-surface temperature may reduce the spray temperature, and therefore potentially generate more freezing, other more important factors like high waves or the occurrence of showers transpire in areas with higher SSTs.

- Icing in Arctic-Norwegian waters occurs most frequently in weather situations with cold-air outbreaks from the ice. However, around 10% of the icing events ensue in mountain-wave conditions offshore of Northern Norway or the Svalbard archipelago. Polar-low conditions may favour the appearance of severe icing, due to the appearance of strong winds, high waves, low temperatures, and heavy snow fall in such conditions.

- Applying thresholds of $T_{850} \leq -15$ °C and $\Delta T_{850} \leq -4$ °C are suggested for long-term predictions of icing. It is shown that this method is more accurate than applying criteria for $T_{2\mathrm{m}}$ and $V_{10\mathrm{m}}$ for icing predictions.

- Some of the results in this study may be different when using other ship types with different bow shapes and free-board heights than those of the applied ships. Thus, more icing observations from other ship types are needed to confirm the validity of these results for other ships.

- Uncertainty in the modelling and prediction of ship icing is high. Hence, more high-quality observations of sea spray, snow fall, icing, turbulence, and waves are needed in order to investigate the current challenges in more details, and verify the modelling approaches proposed by this and other studies.

Finally, both the short-term and long-term prediction models presented in the study may be incorporated in an ensemble prediction system. For a particular icing-prediction model it is possible to vary both the input parameters and the physical parameterization applied in the model. Such an ensemble prediction system may provide the officer of a ship an early warning a couple of days or even weeks ahead of the risk of icing and the probability of the growth rate of icing. If such information is utilised in the best possible manner, it may provide to be a useful tool for better planning of ship operations in a cold marine climate.

References

Berrisford P, Dee D, Poli P, Brugge R, Fielding K, Fuentes M, Kållberg P, Kobayashi S, Uppala S, Simmons A. 2011. The era-interim archive version 2.0. Shinfield Park, Reading.

Bialek EL. 1966. Handbook of oceanographic tables. Technical report, U.S. Naval Oceanographic Office, Washington, D.C.

Blackmore RZ. 1996. Vessel Icing and Spongy Accretion Modelling. PhD thesis, University of Alberta, Edmonton, Alberta.

Blackmore RZ, Lozowski EP, *et al.* 1994. A heuristic freezing spay model of vessel icing. *Int. J. Offshore Polar Eng* **4**(2): 119–126.

Bolton D. 1980. The computation of equivalent potential temperature. *Monthly weather review* **108**(7): 1046–1053, doi:10.1175/1520-0493(1980)108<1046:TCOEPT>2.0.CO;2, URL `http://dx.doi.org/10.1175/1520-0493(1980)108<1046:TCOEPT>2.0.CO;2`.

Borisenkov Y, Zablockiy G, Makshtas A, Migulin A, Panov V. 1975. On the approximation of the spray-cloud dimensions (In Russian). In: *Arkticheskii i Antarkticheskii Nauchno-Issledovatelskii Institut*, Gidrometeoizdat Leningrad, pp. 121–126.

Borisenkov YP, Panov VV. 1972. Osnovnyye rezultaty i perspektivy issledovaniy gidrometeorologicheskikh usloviy obledeneniya sudov (Primary results and prospects for the investigation of the hydrometeorological conditions of ship icing). Technical Report Trudy No. 298, Arkticheskii i Antarkticheskii Nauchnolssledovatiel'Skii lnstitut, Gidrometeoizdat, Leningrad.

Borisenkov YP, Pchelko IG. 1975. Indicators for forecasting ship icing. Technical report, Cold Regions Research and Engineering Laboratory.

Brown RD, Roebber P. 1985. The ice accretion problem in Canadian waters related to offshore energy and transportation. Technical Report 85–13, Candian Climate Centre, Atmospheric Environment Service.

Chung K, Lozowski E, Zakrzewski W, Gagnon R, Thompson T. 1998. Spraying experiments with a model stern trawler. *Journal of ship research* **42**(4): 260–265.

Chung VKK. 1995. Ship icing and stability. Doctoral thesis, University of Alberta.

Curry JA, Webster PJ. 1999. *Thermodynamics of atmospheres and oceans*, vol. 65. Academic Press.

DeAngelis RM. 1974. Superstructure icing. Mariners Weather Log 18, Nacional Oceanic and Atmospheric Administration (NOAA), Washington D.C.

Dee DP, Uppala SM, Simmons AJ, Berrisford P, Poli P, Kobayashi S, Andrae U, Balmaseda MA, Balsamo G, Bauer P, Bechtold P, Beljaars ACM, van de Berg L, Bidlot J, Bormann N, Delsol C, Dragani R, Fuentes M, Geer AJ, Haimberger L, Healy SB, Hersbach H, Hólm EV, Isaksen L, Kållberg P, Köhler M, Matricardi M, McNally AP, Monge-Sanz BM, Morcrette JJ, Park BK, Peubey C, de Rosnay

P, Tavolato C, Thépaut JN, Vitart F. 2011. The ERA-Interim reanalysis: configuration and performance of the data assimilation system. *Quarterly Journal of the Royal Meteorological Society* **137**(656): 553–597, doi:10.1002/qj.828, URL http://dx.doi.org/10.1002/qj.828.

Defraeye T, Blocken B, Carmeliet J. 2010. CFD analysis of convective heat transfer at the surfaces of a cube immersed in a turbulent boundary layer. *International Journal of Heat and Mass Transfer* **53**(1–3): 297–308, doi:10.1016/j.ijheatmasstransfer.2009.09.029, URL http://www.sciencedirect.com/science/article/pii/S0017931009005109.

Dehghani S, Muzychka Y, Naterer G. 2016a. Droplet trajectories of wave-impact sea spray on a marine vessel. *Cold Regions Science and Technology* **127**: 1 – 9, doi:10.1016/j.coldregions.2016.03.010, URL http://www.sciencedirect.com/science/article/pii/S0165232X16300490.

Dehghani S, Naterer G, Muzychka Y. 2016b. Droplet size and velocity distributions of wave-impact sea spray over a marine vessel. *Cold Regions Science and Technology* **132**: 60 – 67, doi:10.1016/j.coldregions.2016.09.013, URL http://www.sciencedirect.com/science/article/pii/S0165232X16302440.

ECMWF. 2015. User guide to ECMWF forecast products. Technical report, European Centre for Medium-Range Weather Forecasts (ECMWF).

Eide LI. 1983. Environmental conditions in the Barents Sea and near Jan Mayen. Technical report, Norwegian Meteorological Institute.

Ekeberg OC. 2010. State-of-the-art on the marine icing models and observations. Techincal report (confidential) 2010-0745, DNV - Det Norske Veritas.

Erichsen AE. 1892. *Nordlands Trompet, eller Beskrivelse over Nordlands Amt (The Trumpet of Nordland, or Description of the county of Nordland)*. Folkeudg., Aschehoug: Kristiania, URL http://urn.nb.no/URN:NBN:no-nb_digibok_2007101703001. Originally written around 1675-1695 by Petter Dass.

Fairall C, Bradley E, Hare J, Grachev A, Edson J. 2003. Bulk parameterization of air-sea fluxes: Updates and verification for the COARE algorithm. *Journal of Climate* **16**(4): 571–591, URL http://dx.doi.org/10.1175/1520-0442(2003)016<0571:BPOASF>2.0.CO;2.

Finstad KJ. 1995. Collision Efficiencies of Drizzle-Size Drops. Technical report, U.S. Army Cold Regions Research and Engineering Laboratory.

Foken T, Nappo CJ. 2008. *Micrometeorology*. Springer Science & Business Media, ISBN 9783540746652.

Forest TW, Lozowski EP, Gagnon RE. 2005. Estimating marine icing on offshore structures using RIGICE04. In: *Proceedings of 11th International Workshop on Atmospheric Icing of Structures*. Montreal, Quebec, pp. 1–9, URL http://nparc.cisti-icist.nrc-cnrc.gc.ca/npsi/ctrl?action=

rtdoc&an=8894858&lang=en.

Gulev SK, Hasse L. 1998. North Atlantic wind waves and wind stress fields from voluntary observing ship data. *Journal of physical oceanography* **28**(6): 1107–1130, doi:10.1175/1520-0485(1998)028<1107:NAWWAW>2.0.CO;2, URL http://dx.doi.org/10.1175/1520-0485(1998)028<1107:NAWWAW>2.0.CO;2.

Günther H, Hasselmann S, Janssen PA. 1992. The WAM model cycle 4. Technical report, Deutsches Klimarechenzentrum (DKRZ).

Hansen ES. 2012. Numerical modelling of marine icing on offshore structures and vessels. Master's thesis, NTNU - Norwegian University of Science and Technology. [Available online at http://hdl.handle.net/11250/246746. Accessed 29 June 2017.].

Hansen ES, Teigen SH. 2015. An efficient numerical model for marine icing. In: *Proceedings of the 23rd International Conference on Port and Ocean Engineering under Arctic Conditions*, 150. Norwegian University of Science and Technology, Trondheim, pp. 1–15. [Available online at http://www.poac.com/Papers/2015/pdf/poac15Final00150.pdf. Accessed 29 June 2017.].

Henry NL. 1995. Forecasting vessel icing due to freezing spray in Canadian east coast waters. Part I: Model physics. Technical report, Environment Canada, Newfoundland Weather Centre.

Horjen I. 1990. Numerical modelling of time-dependent marine icing, anti-icing and de-icing. Doctoral thesis, NTH - Norges Tekniske Høgskole.

Horjen I. 2013. Numerical modeling of two-dimensional sea-spray icing on vessel-mounted cylinders. *Cold Regions Science and Technology* **93**: 20–35, doi:10.1016/j.coldregions.2013.05.003, URL http://www.sciencedirect.com/science/article/pii/S0165232X13000773.

Horjen I. 2015. Offshore drilling rig ice accretion modeling including a surficial brine film. *Cold Regions Science and Technology* **119**: 84 – 110, doi:10.1016/j.coldregions.2015.07.006, URL http://www.sciencedirect.com/science/article/pii/S0165232X15001652.

Horjen I, Carstens T. 1989. Numerical Modelling of Sea Spray Icing on Vessels. In: *Proceedings of the 10th International Conference on Port and Ocean Engineering under Arctic Conditions*. pp. 694–704. [Available online at http://www.poac.com/Papers/POAC89_V2_all.pdf. Accessed 29 June 2017.].

Horjen I, Loeset S, Vefsnmo S. 1986. Icing hazards on supply vessels and stand-by boats. Technical report, Norwegian Hydrotechnical Labratory.

Hyndman RJ, Koehler AB. 2006. Another look at measures of forecast accuracy. *International journal of forecasting* **22**(4): 679–688, doi:10.1016/j.ijforecast.2006.03.001, URL http://www.sciencedirect.com/science/article/pii/S0169207006000239.

Jessup RG. 1985. Forecast techniques for ice accretion on different types of marine

structures, including ships, platforms and coastal facilities. Technical report, World Meteorlogical Organization.

Jones K, Claffey KJ. 2015. Observations and modeling of sea splash icing. In: *Proceedings of IWAIS XV*.

Jones KF, Andreas EL. 2012. Sea spray concentrations and the icing of fixed offshore structures. *Quarterly Journal of the Royal Meteorological Society* **138**(662): 131–144, doi:10.1002/qj.897, URL http://dx.doi.org/10.1002/qj.897.

Kachurin LG, Gashin LI, Smirnov IA. 1974. Icing rate of small displacement fishing boats under various hydrometeorological conditions. *Meteorologiya i Gidrologiya* **3**: 50–60. Moscow.

Kulyakhtin A. 2014. Numerical Modelling and Experiments on Sea Spray Icing. PhD thesis, NTNU - Norwegian University of Science and Technology. [Available online at http://hdl.handle.net/11250/277036 Accessed 29 June 2017.].

Kulyakhtin A, Kulyakhtin S, Loset S. 2016. The role of the ice heat conduction in the ice growth caused by periodic sea spray. *Cold Regions Science and Technology* **127**: 93 – 108, doi:http://dx.doi.org/10.1016/j.coldregions.2016.04.001, URL http://www.sciencedirect.com/science/article/pii/S0165232X16300532.

Kulyakhtin A, Shipilova O, Libby B, Løset S. 2012. Full-scale 3D CFD simulation of spray impingement on a vessel produced by ship-wave interaction. In: *The 21st IAHR International Symposium on Ice*. Dalian, China, pp. 1129–1141.

Kulyakhtin A, Tsarau A. 2014. A time-dependent model of marine icing with application of computational fluid dynamics. *Cold Regions Science and Technology* **104–105**(0): 33–44, doi:10.1016/j.coldregions.2014.05.001, URL http://www.sciencedirect.com/science/article/pii/S0165232X14000962.

Lien VS, Gusdal Y, Albretsen J, Melsom A, Vikebø FB. 2013. Evaluation of a Nordic Seas 4km numerical ocean model hindcast archive (SVIM), 1960-2011. Research report, Institute of Marine Research.

Lienhard IV JH, Lienhard V JH. 2008. *A Heat Transfer Textbook*, vol. 3. Phlogiston Press.

Løset S, Shkinek KN, Gudmestad OT, Høyland KV. 2006. Icing in the Ocean. In: *Actions from ice on arctic offshore and coastal structures*, ch. 6, LAN: St. Petersburg, pp. 191–206. Student's Books for Institutes of Higher Education. Special Literature.

Lozowski EP, Stallabrass JR, Hearty PF. 1983. The icing of an unheated, non-rotating cylinder. Part I: A simulation model. *Journal of climate and applied meteorology* **22**(12): 2053–2062.

Lozowski EP, Szilder K, Makkonen L. 2000. Computer simulation of marine ice accretion. *Philosophical Transactions of the Royal Society of London. Series*

A: Mathematical, Physical and Engineering Sciences **358**(1776): 2811–2845, doi:10.1098/rsta.2000.0687.

Lundqvist J, Udin I. 1977. Ice accretion on ships with special emphasis on Baltic conditions. Research Report 23, Winter Navigation Research Board, Swedish Administration of Shipping and Navigation, Finnish Board of Navigation., Norrköping, Sweden.

Makkonen L. 1984a. Atmospheric icing on sea structures. Technical report, DTIC Document.

Makkonen L. 1984b. Modeling of Ice Accretion on Wires. *Journal of Climate and Applied Meteorology* **23**(6): 929–939, doi:10.1175/1520-0450(1984)023<0929:MOIAOW>2.0.CO;2, URL http://dx.doi.org/10.1175/1520-0450(1984)023<0929:MOIAOW>2.0.CO;2.

Makkonen L. 1987. Salinity and growth rate of ice formed by sea spray. *Cold Regions Science and Technology* **14**(2): 163–171, doi:10.1016/0165-232X(87)90032-2, URL http://www.sciencedirect.com/science/article/pii/0165232X87900322.

Makkonen L. 2010. Solid fraction in dendritic solidification of a liquid. *Applied Physics Letters* **96**(9), doi:10.1063/1.3306728, URL http://scitation.aip.org/content/aip/journal/apl/96/9/10.1063/1.3306728.

Makkonen L, Brown RD, Mitten PT. 1991. Comments on "Prediction of vessel icing for near-freezing sea temperatures". *Weather and Forecasting* **6**: 565–567.

Makkonen L, Fujii Y. 1993. Spacing of icicles. *Cold regions science and technology* **21**(3): 317–322.

MAROFF. 2013. Optimization of ship operations in Arctic waters by application of sensor technologies for ice detection, de-icing and weather data. Project description.

Mertins HO. 1968. Icing on fishing vessels due to spray. *Marine Observer* **38**(221): 128–130.

Mesinger F, DiMego G, Kalnay E, Mitchell K, Shafran PC, Ebisuzaki W, JoviÄĞ D, Woollen J, Rogers E, Berbery EH, Ek MB, Fan Y, Grumbine R, Higgins W, Li H, Lin Y, Manikin G, Parrish D, Shi W. 2006. North American Regional Reanalysis. *Bulletin of the American Meteorological Society* **87**(3): 343–360, doi:10.1175/BAMS-87-3-343, URL http://dx.doi.org/10.1175/BAMS-87-3-343.

MET Norway. 2015. Text forecast for high seas. Accessed 4 December 2015. Electronic, URL http://www.yr.no/hav_og_kyst/tekstvarsel/hav/.

Müller M, Homleid M, Ivarsson KI, Køltzow MAØ, Lindskog M, Midtbø KH, Andrae U, Aspelien T, Berggren L, Bjørge D, Dahlgren P, Kristiansen J, Randriamampianina R, Ridal M, Vignes O. 2017. AROME-MetCoOp: A Nordic Convective-Scale Operational Weather Prediction Model. *Weather and Forecasting* **32**(2): 609–627, doi:10.1175/WAF-D-16-0099.1, URL https://doi.

org/10.1175/WAF-D-16-0099.1.

Naseri M. 2016. RAM Analysis of Oil and Gas Production Facilities Operating in the Arctic offshore: Expert Judgements and Operating Conditions. PhD thesis, UiT - The Arctic University of Norway. [Available online at http://hdl.handle.net/10037/9972. Accessed 29 June 2017.].

NCEP. 2017. Global Forecast System (GFS). URL http://www.emc.ncep.noaa.gov/GFS/.php. Accessed 12 June 2017.

Noer G, Lien T. 2010. Dates and positions of polar lows over the Nordic Seas between 2000 and 2010. Met. no Report 16, Norwegian Meteorological Institute.

Nordeng TE, Rasmussen EA. 1992. A most beautiful polar low. A case study of a polar low development in the Bear Island region. *Tellus A* **44**(2): 81–99.

Norwegian Maritime Authority. 2014. Ulykkesdatabase (Database of ship incidents). [Available online at https://www.sjofartsdir.no/ulykker-sikkerhet/ulykkesstatistikk/datauttrekk/. Accessed 29 August 2016.].

Nygaard BE, Ágústsson H, Somfalvi-Tóth K. 2013. Modeling wet snow accretion on power lines: improvements to previous methods using 50 years of observations. *Journal of Applied Meteorology and Climatology* **52**(10): 2189–2203.

Overland JE. 1990. Prediction of vessel icing for near-freezing sea temperatures. *Weather and Forecasting* **5**: 62–77, doi:10.1175/1520-0434(1990)005<0062:POVIFN>2.0.CO;2, URL http://dx.doi.org/10.1175/1520-0434(1990)005<0062:POVIFN>2.0.CO;2.

Overland JE. 1991. Reply. *Weather and Forecasting* **6**(4): 568–570.

Overland JE, Pease CH, Preisendorfer RW, Comiskey AL. 1986. Prediction of vessel icing. *Journal of Climate and Applied Meteorology* **25**(12): 1793–1806, doi:10.1175/1520-0450(1986)025<1793:POVI>2.0.CO;2, URL http://dx.doi.org/10.1175/1520-0450(1986)025<1793:POVI>2.0.CO;2.

Panov VV. 1971. On the frequency of splashing a medium-sized fishing vessel with sea spray (in Russian). In: *Theoretical and Experimental Investigations of the Conditions of Icing of Ships*, Gidrometeoizdat Leningrad, pp. 87–90.

Panov VV. 1978. Icing of ships. In: *Polar Geography*, vol. 2, Taylor & Francis, pp. 166–186, doi:10.1080/10889377809388652, URL http://dx.doi.org/10.1080/10889377809388652.

Pease CH, Comiskey AL. 1985. Vessel icing data in Alaskan waters-1979-1984 dataset. NOAA Data Report ERL PMEL-14, Pacific Marine Environmental Laboratory.

Pierson WJ, Moskowitz L. 1964. A proposed spectral form for fully developed wind seas based on the similarity theory of sa kitaigorodskii. *Journal of geophysical research* **69**(24): 5181–5190.

Rashid T, Khawaja H, Edvardsen K. 2016. Determination of Thermal Properties of Fresh Water and Sea Water Ice using Multiphysics Analysis. *Interna-*

tional Journal of Multiphysics **10**(3), doi:10.21152/1750-9548.10.3.277, URL http://journal.multiphysics.org/index.php/IJM/article/download/81/pdf.

Rasmussen R, Baker B, Kochendorfer J, Meyers T, Landolt S, Fischer AP, Black J, Thériault JM, Kucera P, Gochis D, *et al.* 2012. How well are we measuring snow: The NOAA/FAA/NCAR winter precipitation test bed. *Bulletin of the American Meteorological Society* **93**(6): 811–829.

Rasmussen RM, Vivekanandan J, Cole J, Myers B, Masters C. 1999. The Estimation of Snowfall Rate Using Visibility. *Journal of Applied Meteorology* **38**(10): 1542–1563, doi:10.1175/1520-0450(1999)038<1542:TEOSRU>2.0.CO;2, URL https://doi.org/10.1175/1520-0450(1999)038<1542:TEOSRU>2.0.CO;2.

Reistad M, Breivik Ø, Haakenstad H, Aarnes OJ, Furevik BR, Bidlot JR. 2011. A high-resolution hindcast of wind and waves for the North Sea, the Norwegian Sea, and the Barents Sea. *Journal of Geophysical Research: Oceans (1978–2012)* **116**(C5), doi:10.1029/2010JC006402, URL http://dx.doi.org/10.1029/2010JC006402.

Roebber P, Mitten P. 1987. Modelling and measurement of icing in Canadian waters. Technical report, Canadian Climate Centre, Atmospheric Environment Service.

Rohsenow WM, Choi HY. 1961. *Heat, mass, and momentum transfer*. Prentice Hall.

Ryerson CC. 1995. Superstructure spray and ice accretion on a large U.S. Coast Guard cutter. *Atmospheric Research* **36**(3–4): 321–337, doi:10.1016/0169-8095(94)00045-F, URL http://www.sciencedirect.com/science/article/pii/016980959400045F.

Ryerson CC, Gow AJ. 2000. Crystalline structure and physical properties of ship superstructure spray ice. *Philosophical Transactions of the Royal Society of London A: Mathematical, Physical and Engineering Sciences* **358**(1776): 2847–2871, doi:10.1098/rsta.2000.0688.

Ryerson CC, Longo PD. 1992. Ship Superstructure Icing: Data Collection and Instrument Performance on USCGC Midgett Research Cruise. Technical report, DTIC Document.

Samuelsen EM. 2007. Et dynamisk studium av stormen Narve - et kaldluftsutbrudd i Finnmark - ved hjelp av observasjoner og numeriske simuleringer. (A dynamical study of the storm Narve - a cold air outbreak in Finnmark - with the use of observations and numerical simulations.). Master's thesis, University of Bergen, Bergen.

Sawada T. 1962. Icing on ships and the forecasting method.(In Japanese). *Snow and Ice* (24): 12–14.

Sawada T. 1967. A forecasting method for ship icing near the Kuril Islands (In

Japanese). *J. Met. lies., JMA* **18**.

Sawada T. 1968. Ice accretion on ships in northern seas of Japan. *J. Meteorol, Soc. Japan* **46**: 350–354.

Shchepetkin AF, McWilliams JC. 2005. The regional oceanic modeling system (ROMS): a split-explicit, free-surface, topography-following-coordinate oceanic model. *Ocean Modelling* **9**(4): 347–404.

Shellard HC. 1974. The meteorological aspects of ice accretion on ships. Technical Report 10, World Meteorological Organization. Marine Science Affairs Report.

Stallabrass J. 1979a. Icing of fishing vessels: An analysis of reports from Canadian east coast waters. National Research Council Canada. Technical report, Laboratory Technical Report LTR-LT-98.

Stallabrass JR. 1979b. The concentration of falling snow and its relations to visbility. In: *Transportation*, vol. 11, National Research Council Canada, Division of Mechanical Engineering: Ottawa, Canada. ISSN 0381-4963.

Stallabrass JR. 1980. Trawler icing - A compilation of work done at N.R.C. Mechanical Engineering Report MD-56, National Research Council Canada.

Stull RB. 1988. *An introduction to Boundary Layer Meteorology*, vol. 13. Springer Science & Business Media, ISBN 9027727694.

Süld J, Dale KS, Myrland E, Batrak Y, Homleid M, Valkonen T, Seierstad IA, Randriamampianina R. 2016. AROME-Arctic: New operational NWP model for the Arctic region. In: *EGU General Assembly Conference Abstracts*, vol. 18. p. 14429.

Teigen SH, Hansen ES, Roth JC. 2015. Marine icing severity in the Barents sea. In: *Proceedings of the 23rd International Conference on Port and Ocean Engineering under Arctic Conditions*, 148. Norwegian University of Science and Technology, Trondheim, pp. 1–7. [Available online at `http://www.poac.com/Papers/2015/pdf/poac15Final00148.pdf`. Accessed 29 June 2017.].

The Seattle Times. 2017. Memorial fund for crew lost in Bering Sea gets help from 'Deadliest Catch' captain. Electronic. Journalist Hal Bernton. Accessed 02 June 2017. `http://bit.ly/2nNa9Vp`.

Tolman H. 2014. The WAVEWATCH III Development Group. User Manual and System Documentation of WAVEWATCH III version 4.18. Technical report, Nacional Oceanic and Atmospheric Administration (NOAA).

United States Coast Guard. 2008. Report of investigation into the sinking and loss of four crewmembers aboard the commercial fishing vessel Lady of Grace. Technical report, United States Coast Guard, Washington D.C. [Available online at `http://www.uscg.mil/hq/cg5/cg545/docs/documents/LadyOfGrace.pdf`. Accessed 6 March 2017.].

Utaaker K. 1975. Frost Smoke Downstream of Hydroelectric Power Plants. In: *In commemoration of the 60th birthday of Prof. A.Baumgartner. A collection.*, Univ. Munich, Met. Inst., pp. 206–210.

Vasilyeva GV. 1971. Gidrometeorologicheskiye usloviya obledeniya morskikh sudov. (Hydrometeorological conditions of the icing of sea-going ships.). T. Vyp, 87, Gidromet. Nauo-Issled. Centre SSSR, Leningrad.

Wise JL, Comiskey AL. 1980. Superstructure icing in Alaskan Waters. NOAA Special Report, Pacific Marine Evironmental Laboratory.

WMO. 1962. Commission for Synoptic Meteorology abridged final report of the third session. General summary. Rec. 26-28 CSM-III (Mar. 1962). WMO Report No.122. Rp.50, World Meteorological Organization (WMO). [Available online at https://www.wmo.int/pages/prog/amp/mmop/documents/publications-history/cbs/CSM03Rec26-28.pdf. Accessed 29 August 2016.].

Wu J, Murray JJ, Lai RJ. 1984. Production and distributions of sea spray. *Journal of Geophysical Research: Oceans* **89**(C5): 8163–8169, doi:10.1029/JC089iC05p08163, URL http://dx.doi.org/10.1029/JC089iC05p08163.

yrno. 2017a. Her kjemper soldatene mot isen (Here the soldiers fight against the ice). URL http://www.yr.no/artikkel/her-kjemper-soldatene-mot-isen-1.13471313. By journalist Astrid Rommetveit. Accessed 10 June 2017.

yrno. 2017b. Kart over fiskebankene (Map of fishing banks). Electronic, URL http://www.yr.no/hav_og_kyst/kart_over_fiskebankene. Accessed 06 June 2017.

Zakrzewski W, Lozowski E. 1987. The application of a vessel spraying model for predicting the ice growth rates and loads on a ship. In: *Proceedings of the 9th International Conference on Port and Ocean Engineering under Arctic Conditions*, vol. 3. Fairbanks, pp. 591–603.

Zakrzewski WP. 1986. Icing of ships, part 1: Splashing a ship with spray. Technical report, NOAA - National Oceanic and Atmospheric Administration.

Zakrzewski WP. 1987. Splashing a ship with collision-generated spray. *Cold Regions Science and Technology* **14**(1): 65–83, doi:10.1016/0165-232X(87)90045-0, URL http://www.sciencedirect.com/science/article/pii/0165232X87900450.

Zakrzewski WP, Blackmore R, Lozowski EP. 1988a. Mapping icing rates on sea-going ships. *Journal of the Meteorological Society of Japan* **66**(5): 661–675.

Zakrzewski WP, Lozowski EP. 1989. Soviet marine icing data. Technical report, Canadian Climate Centre, Atmospheric Environment Service.

Zakrzewski WP, Lozowski EP, Horjen I. 1989. The use of ship icing models for forecasting icing rates on sea-going ships. In: *Proceedings of the 10th International Conference on Port and Ocean Engineering under Arctic Conditions*. Luleå University of Technology, pp. 1454–1467. [Available online at http://www.poac.com/PapersOnline.html. Accessed 29 June 2017.].

Zakrzewski WP, Lozowski EP, Muggeridge D. 1988b. Estimating the extent of the

spraying zone on a sea-going ship. *Ocean Engineering* **15**(5): 413 – 429, doi: 10.1016/0029-8018(88)90008-X, URL http://www.sciencedirect.com/science/article/pii/002980188890008X.

Zakrzewski WP, Lozowski EP, Thomas W, Bourassa M, Blackmore R, Szilder K, Kobos A. 1993. A three-dimensional time-dependent ship icing model. In: *Proceedings of the 12th International Conference on Port and Ocean Engineering under Arctic Conditions*. Hamburg, pp. 857–873. [Available online at http://www.poac.com/PapersOnline.html. Accessed 29 June 2017.].

Part II
Appended papers